YEAR 3

DEVELOPMENT OF PERMEABLE REACTIVE BARRIER FOR CHROMIUM RESIDUE SITES IN NEW JERSEY

Final Report

By

M. E. Labib, S. S. Dukhin and J. Schuring
New Jersey Institute of Technology
Newark, NJ 07102

Submitted to:

Dr. Paul Sanders
New Jersey Department of Environmental Protection
Division of Science, Research & Technology
Trenton, NJ 08625

May 11, 2001

ACKNOWLEDGEMENTS

The authors express their appreciation to Dr. Paul Sanders for his support, guidance and insight during this research program. We wish to thank NJ DEP for supporting this research over the past three years and hope that the results will be used to remediate groundwater at the Hudson County sites.

On behalf of the graduate students, we express our gratitude to NJ DEP and NJIT for their financial support.

We extend our thanks to Teruo Sugihara and Frank Faranca for their contribution and support.

We would also like to thank the responsible parties for supplying us with groundwater as well as information regarding the sites.

TABLE OF CONTENTS

	Page No.
Acknowledgements	ii
Table of Contents	iii
Executive Summary	iv
1. Introduction	1
2. Experimental Procedures	3
3. Reactive Media Capacity and Prediction of PRB Lifetime	5
4. Results and Discussion	10
5. Barrier Design and Prevention of Groundwater Streamlining	16
6. Different Variants of Barrier Hydrological Design	23
7. Quality Assurance	24
8. Conclusions and Recommendations for Future Research	26
9. Recommendations and Application and Use by NJDEP	26
References	27
Figures	30
Appendices	46

EXECUTIVE SUMMARY

This research program addressed the development of permeable reactive barrier (PRB) technology for treating chromium-contaminated groundwater at sites located in Hudson County, New Jersey. The effort involved the development of new reactive media (RM) with high reductive capacity for Cr(VI), experimental methodology and models to define the basic design requirements of PRBs for use at three sites.

The sites were selected to cover a range of pH, chromium concentration, and groundwater velocity. Such sites should therefore represent other sites in New Jersey and elsewhere. The main challenge was to develop high capacity reactive media for treating groundwater with high pH values (>11.0), where the conventional iron (Fe^0) is not suitable for use in PRBs under these conditions. This is due to the rapid formation of a thick passivating layer on the surface of iron particles at high pH. New strategies to overcome the high pH problem were developed, notably with the use of acid-producing reactive media that can operate successfully over a long time to treat high-pH groundwater.

Another significant challenge was to develop new methods to measure reactive media capacity values that are relevant for predicting long-term application in PRBs. Quantitative capacity value is needed to estimate the thickness of a barrier for each of the sites based on groundwater velocity and chromium concentration.

Notably, models were developed to define barrier thickness based on the hydraulic conductivity, groundwater velocity and reactive media capacities for each of the sites. Predictions of PRB thickness were made for each of the three sites based on thirty-year service life. These exact models are critical to successfully applying this technology. In addition, elaborate modeling efforts were completed to address issues of bypassing and define the important design issues that may be encountered during the implementation of this technology.

The work has resulted in many original contributions in groundwater treatment, especially for chromium reprocessing waste sites. Five Masters theses were produced during this research and several publications are under preparation. The information given in this report is supplemented with several appendices and copies of theses. These documents should be archived for future use regarding the remediation of groundwater at chromium ore processing residue (COPR) sites in New Jersey.

The following are key results of this research program:

1. The reactive media capacities (C_{RM} or RMC expressed in mg Cr/cm^3) of four reactive iron media (Fe^0), iron (Fe^0)-pyrite and iron (Fe^0)-siderite mixtures were evaluated by the "thin plug" experimental method developed at NJIT during this research. The RMC of iron at high pH is very low and has been found to be insufficient for use in PRB for the case of NJ sites. The C_{RM} of iron-pyrite mixture (IPM, 50/50) and iron-siderite mixtures were found to be more than 10 times larger than that of conventional reactive iron.
2. In all experiments the strong dependence of the RM capacity on the groundwater (GW) velocity has been strongly manifested. The capacity increased more than an order of magnitude by decreasing the groundwater velocity (u_c) to a level similar to that at the sites. Consequently, the use of similar velocities (to that in the barrier) in the laboratory experiments is an essential condition for modeling chromium removal within a barrier. Therefore, in order to arrive at an accurate value of RMC the experiments had to be conducted at low groundwater velocity and for a long period of time (> 1 year in some cases). We found that the smaller velocity and correspondingly the longer time of chromium

accumulation result in larger RMC values. On the one hand, C_{RM} value for IPM in the first set of experiments with 3-month duration was about 20 mg/cm^3. On the other hand, 36 mg/cm^3 was accumulated during a second set of experiments with duration about 12 months.

3. IPM stability, i.e. number of pore volume (NPV) at pH about 12 (2300 at Cr concentration 16 ppm and u_c = 54 m/year) is almost 30 times better than iron stability (80 at Cr concentration 18 ppm and u_c = 40 m/year) at pH about 7 (16). This means that IPM is a much better RM for pH=12 compared to iron (Fe^0) at pH about 7-9. Consequently, IPM is a suitable RM for groundwater remediation under the most difficult conditions: larger GW velocities, higher Cr concentrations and higher pH.
4. For predicting the service life of a barrier, a three-layer dynamic model describing the distribution of accumulated chromium within the barrier has been developed. The chromium accumulated during treatment fills the front part of the barrier almost completely with the preservation of fresh RM layer near barrier back surface. The first layer can be called accumulation layer. The third layer adjacent to barrier back surface does not contain chromium (contains only fresh RM). The second layer located between first and third, is referred to as chromium treatment layer because the reduction takes place within this layer. According to this model, there is always a slow residual reduction within the first layer at any time and there is no substantial reduction in the third layer because Cr(VI) has been reduced and accumulated as Cr(III) within the second layer. The concentration profile (of accumulated chromium) and the thickness of the second layer "almost" do not change with time. The thickness of this treatment layer is small in comparison with the entire barrier thickness, d_b. Therefore, the entire amount of chromium accumulated within a barrier can be identified by that accumulated within the first layer when its thickness approaches that of the entire barrier. The effluent concentration starts to increase when the third layer eventually disappears.
5. Two steps need to be discriminated regarding the kinetics of chromium accumulation within a section of the barrier: the first step resulting in almost zero effluent concentration and the second step resulting in monotonous increase of effluent concentration. Correspondingly, the total capacity C_{RM}^{tot} may be introduced, in addition to C_{RM}. According to our modeling and experimental results, the universally accepted NPV underestimates the barrier lifetime because the total capacity of RM is not accounted for. This underestimation occurs because C_{RM} only accounts for the amount of chromium accumulated according to the NPV notion (first step) and thus it ignores the amount accumulated during the second step. The generalized equation for barrier lifetime C_{RM}^{tot} has been derived with respect to the above proposed model which accounts for the two-stage chromium accumulation in the barrier space.
6. Hydraulic conductivity (HC) of iron-pyrite mixture (IPM - no sand added) is smaller than that of the aquifer because the pyrite particle dimension is rather small (40 micron). Consequently, this RM (iron-pyrite) may be used as a mixture with coarse sand in order to avoid bypassing around the barrier. The phenomenon of gravitational segregation is observed during dry mixing of pyrite, sand and iron because pyrite particle dimension is smaller than the pores between adjacent coarse sand particles. A rather uniform mixture of RM with coarse sand was achieved by wet mixing. HC of the iron-pyrite-sand mixture was measured as a function of RM volume fraction. RM volume fraction of 0.2 may be recommended because at larger RM content the HC decrease is large. Barrier bypassing may be eliminated with the use of iron-pyrite-sand mixture because aquifer HC of the 3 sites is

smaller than that of coarse sand. However, the capacity for chromium removal per cm^3 decreases with the sand content in the mixture.

7. A significant enhancement of chromium removal for RM mixed with sand was found to be in agreement with the experimental data of Powell *et al.* (7). IPM capacity in the presence of sand is about 80 mg per cm^3 of RM. The reactive capacity for the mixture of sand with iron-pyrite RM at volume fraction of 0.2 is 16 mg/cm^3. This value is used to evaluate the barrier thickness necessary for chromium accumulation during 30 years.
8. A complete analysis of the modes of groundwater flow was performed with account for difference in HC of waste depository and surrounding soil. Because of this difference in HC, GW does not flow along a straight line as it is assumed in the conventional case of a barrier bypassing with GW. There is a convergent GW flow before waste depository (WD) if its hydraulic conductivity, K_w exceeds that of the surrounding soil, K_s. The capture width and correspondingly the barrier critical thickness can increase by a factor of 2 at large K_w condition. There is a divergent flow before WD if $K_w < K_s$. The capture width and correspondingly critical barrier thickness d_{bcr} decrease proportional to K_s. The measurement of K_w/K_s ratio for every WD (site) is important. A method is proposed to define the hydrodynamic field around a waste depository for the contaminated sites.
9. In the case of convergent flow, a larger amount of GW crosses the barrier and correspondingly larger amount of chromium has to be accumulated in such a barrier; a large barrier thickness is thus required. In this case a large amount of RM has to be incorporated in the barrier if the depository HC exceeds that of the surrounding soil. On the contrary, for divergent flow a smaller amount of GW crosses the barrier and its thickness may be smaller.
10. The predicted barrier thickness necessary for remediating GW for the Allied Signal and P.P.G sites is estimated to be about 1 meter (or less) for 30 years service life. The prediction is based on the 3-layer model for the chromium accumulation within barrier. The barrier may be represented as a sequence of thin layers. Any layer during 30 years accumulates approximately the same amount of chromium equivalent to our thin-plug experiment of the same thickness during 1 year.
11. The predicted barrier thickness for C.L.H. site is 1.8 m if the depository HC equals to that of the surrounding aquifer and 3.6 m if the depository HC is much larger than that of the aquifer. To accurately estimate these thicknesses, measuring the HC of the waste depository and surrounding aquifer is necessary.

1. INTRODUCTION

1.1 Permeable Reactive Barrier

A permeable reactive barrier (PRB) is a passive treatment zone of reactive material that degrades or immobilizes contaminants as groundwater flows through it (Figure 1.1). The contaminants in groundwater react with the reactive media where they are transformed into harmless precipitates within such a barrier (1,2). Being passive, the barrier does not require any power or maintenance for a long period of time. The application of this permeable reactive barrier requires a thorough knowledge of the reactivity of reactive media in the barriers with the specific contaminant present in the groundwater. In this study, we are concerned with the treatment of chromium-contaminated groundwater, specifically for the case of chromium refining waste sites located in Hudson County, New Jersey.

The selection of reactive media for chromate removal with permeable reactive barriers from groundwater under alkaline conditions (pH about 12) needs to be investigated as most of the chromium-contaminated sites in New Jersey have high pH.

The main objective of this research was to select the best reactive medium (RM) to be used in PRB to treat chromate-contaminated groundwater (GW) under the high alkaline conditions present at New Jersey sites. The study was carried out with the following objectives:

1. To study the performance of elemental iron (Fe^0) at pH > 11.0.
2. To assess pyrite and siderite minerals as reduction media under the high pH conditions (>11.0).
3. To determine the reactive capacities of Fe^0-pyrite and Fe^0-siderite mixtures at high pH (>11.0).
4. To determine their reactive capacity in the mixture with the coarse sand.
5. To combine the generated information with existing literature and to evaluate models, especially with respect to assessment of long-term performance and passivation of RM within PRB.
6. To evaluate the barrier critical thickness necessary for 30 years active life for the three COPR (chromium ore processing residue) sites in New Jersey.

1.2 Oxidation States of Chromium and Mechanism of Chromate Reduction

Chromium is a commonly identified groundwater contaminant. It is present in nature mostly as chromite ore, with a nominal composition of $FeO.Cr_2O_3$ (3). Chromium present in the chromite ore is in the trivalent state, Cr(III). The other most common valence state of chromium is hexavalent, Cr(VI). Oxidation potential and pH of the environment are the two most important factors determining the ratio of the two common valence states (Cr(III)/Cr(VI)) in any physical system.

Hexavalent chromium species are stable in an oxidizing atmosphere, whereas the trivalent species dominate in a reducing environment (4). At pH>6, Cr can exist as chromate ion, CrO_4^{2-}. Despite the strong adsorption affinity of chromate ion to certain mineral surfaces, it is mobile in subsurface systems compared to Cr (III) species (5). Due to its mobility, chromate ion is an environmental concern due to its toxic and carcinogenic properties (4).

Reduction of Cr(VI) by iron, with main focus on ferrous ions in solution, and in the presence of iron bearing minerals are reported in the literature. Gould (6) examined the reduction of Cr(VI) and showed that iron (Fe^0) surfaces are effective in reducing Cr(VI) to Cr(III) under low pH conditions. A corrosion mechanism is proposed to explain this reduction process (7). As iron metal corrodes in water, ferrous ion is produced at local anodic sites, and acid is consumed

by forming hydrogen gas at local cathodic sites (8). Elemental iron (Fe^0) is also used in permeable reactive processes as a means of enhancing abiotic reductive dechlorination of organic compounds (9,10). Reduction of Cr(VI) to Cr(III) occurs rapidly under acidic conditions (11,12). The reduction rate decreases with increasing the pH of groundwater to be treated (13,14,15). Elemental iron (Fe^0) has the potential to induce rapid reduction to Cr(III) which subsequently precipitates to form a mixed Cr(III)-Fe(III) oxyhydroxide (16).

1.3 Iron as Reductive Media for Cr(VI) at Different pH

Iron, as the reductive media for Cr(VI) reduction at different pH, has been studied for its effectiveness in the treatment of contaminated groundwater. Experimental modeling (16,17), barrier installation and post-installation monitoring (18,19) have confirmed that elemental iron is effective in removing CrO_4^{2-} ion from the aqueous phase at intermediate pH conditions. The systematic investigation for chromium reductions with ferrous ions is well known (20,21,22) and is sufficiently rapid (20) at neutral to alkaline pH (7-10). The precipitation of a mixed Cr(III)-Fe(III) oxyhydroxide occurs at pH values between 5-11 (19,21) which generally lowers the total dissolved concentration of Cr(III) less than the drinking water standards of 0.1 ppm. However, formation of the hydroxide complexes results in higher solubilities if the pH is increased above 11 (21). This is often considered as a serious restriction for the treatment of hexavalent chromium at higher pH (>11). Fundamentally the decline in reduced chromium precipitation can occur too at initial pH values lower than 11 because the oxidation of Fe^0 to Fe^{2+} results in increase in pH (7,15), as follows:

$$Fe^0 + 2H^+ + \frac{1}{2}O_2 \Leftrightarrow Fe^{2+} + H_2O \qquad [1.3.1]$$

The pH increase due to chromium reduction and chromium-iron hydroxide formation is confirmed from the following net reaction (7):

$$Fe^0 + CrO_4^{2-} + 4H_2O \Leftrightarrow Fe(OH)_3 + Cr(OH)_3 + 2OH^- \qquad [1.3.2]$$

As the moderate pH is more favorable for chromium removal, the application of ferrous (Fe^{2+}) bearing minerals, such as pyrite and siderite, is well known. Prior to this study, there was no systematic investigation of Cr(VI) reduction with the use of elemental iron (Fe^0) at extreme high pH (>11).

1.4 Pyrite as a Reductive Media for Cr(VI) at Different pH

Pyrite is used as RM for moderating the pH of contaminated groundwater (23,24). The oxidation of pyrite produces acid, which offsets the acid consumed during the oxidation of Fe^0. In the presence of oxygen, the net reaction of pyrite oxidation is as follows:

$$FeS_2 + \frac{7}{2}O_2 + H_2O \Leftrightarrow Fe^{2+} + 2H^+ + 2SO_4 \qquad [1.4.1]$$

Desai (38) showed that these minerals even under high pH conditions have lowered chromium concentrations. Also the Cr(VI) reduction with pyrites in the absence of oxygen is increased due to the production of acids, as shown in Eq. [1.4.1]. There is no systematic investigation of Cr(VI) reduction with the use of pyrite at high alkaline pH. Reduction of Cr(VI) with pyrite under highly alkaline pH condition is a major part of this research.

1.5 Chromite Ore Processing Residue (COPR)

The industrial conversion of Cr(III) in chromite ore to the soluble hexavalent form is called the chromium refining process. This process is accomplished by roasting the chromite ore in the presence of soda ash, lime and air at about 1100-1150 °C, and thereby converting the trivalent chromium to water-soluble chromate i.e., Cr(VI). The yield of this process is usually between 65% to 85% based on the content of chromium in the ore (25,26). Mixed Cr(III)-Cr(VI) solid residue waste is generated from this high temperature kiln process. This residue is alkaline in nature since lime and soda ash are used in this process. Earlier in the century, such residue was landfilled in sites near the production facilities. The ratio of Cr(III) to Cr(VI) in refining wastes varied depending on the original nature of the residue, production process, pH and other transformations that may have taken place since landfilling (27,28,29). Because of these reasons, soluble Cr(VI) species from these landfills have been found to significantly contaminate groundwater in the vicinity of these sites (30). That is why it is necessary to develop a technology to treat groundwater with high pH values (>11).

2. EXPERIMENTAL PROCEDURES

The groundwater samples were obtained from extraction wells present at three sites located in Hudson County, New Jersey, namely: Chemical Land Holding (C.L.H.), Allied Signal and P.P.G sites. Table 2.1 summarizes the pH, Eh, and total chromium concentrations of groundwater samples used in this study. The pH of all groundwater of these sites is alkaline and ranges between 11.5 and 12.35. For the evaluation of residence time, Table 2.1 is supplemented with mean values of pore velocity of groundwater within the aquifer at the site, with account for their seasonal variation. Estimation of pore velocity, with the use of groundwater velocity, is done by assuming the field-cell porosity of 0.65 (31). Residence time refers to the duration of time the contaminated groundwater remains in contact with the reactive media in the permeable reactive barrier, assuming the same hydraulic conductivity of barrier as the aquifer.

Table 2.1: Groundwater stream characteristics for three sites of Hudson County

Characteristic	C.L.H.	Allied Signal	P.P.G
Total chromium concentration (ppm)	55	25	16
pH	12.3	12.2	11.5
Eh (mV)	155	167	240
Groundwater velocity (cm/day)	5-26	1.1-3	15
Residence time (hours)	480-92	2200-800	160

2.1 Materials

Two types of reductive iron media, namely Fisher iron and Peerless iron, were used in our experiments. Peerless iron was supplied by the Peerless Iron Company while the Fisher iron was purchased from the Fisher Scientific Company. The Peerless iron was used for the extensive evaluation in this research. Information about the particle dimension of the iron media used in this study is given in Table 2.2. The Peerless iron was used without any pretreatment. Pyrite and siderite minerals used in our experiments were obtained from Chemalloy Company and Scott Resources Company, respectively.

Table 2.2: Information about different types of Peerless iron used in experiments

Iron #1		Iron # 2		Iron # 3	
Mesh size	% retained	Mesh size	% retained	Mesh size	% retained
16	0	50	0	60	0
18	0	60	2	80	0.6
25	7	70	20	100	4
40	42	80	17	325	73.2
50	22	100	25	Pan	22
80	19	120	11		
100	4	Pan	25		
Pan	5				

2.2 Analytical Procedure

A microprocessor-based pH meter with an Eh measuring mode (JENCO model 6071) was used. The pH and the corresponding temperature were measured using a 3-in-1 electrode (pH and reference electrode combined with temperature probe – JENCO model 6000). The pH meter was calibrated with standard solutions of pH 4, 7 and 10. The pH was regularly calibrated before the measurements.

An oxidation-reduction potential (ORP) electrode was used to measure the Eh of the solution. The electromotive force between the potentials on the standard Ag | AgCl reference and the platinum band, which acts as the second electrode, is measured by the combination ORP electrode. The ORP electrode was routinely tested with the quinhydrone standard test solution, as per standard methods.

The total chromium concentration in groundwater samples was analyzed by Atomic Adsorption (AA) spectroscopy. The analysis of samples was carried out using Smith- Heiftje atomic adsorption spectrophotometer. The light source used for the analysis was a hollow cathode lamp with a current of 6.0 mA. The wavelength required is 357.9 nm and with a bandpass of 0.5 nm. The linear range of the instrument was between 0-5μg/ml of total chromium. The total chromium measurement was done following the EPA protocols under method #7000 and method #7191 (32,33). The hexavalent chromium concentrations in the samples were measured by colorimetric analysis based on absorption spectroscopy at 540 nm. The analysis was carried out using the Varian DMS 3000 UV-visible spectrophotometer. The hexavalent chromium was done following the EPA protocols under method #7169A (34). Diphenylcarbazide was used as a coloring agent and the sample was acidified for color development using 10% HCl (vol/vol), as per the standard method.

2.3 Shaken Packed Bed Experiment

The evaluation of reductive systems and reduction rate calculations for different types of iron at pH 12 were done by the shaken packed-bed experiment. In this case, a known quantity of reactive media was mixed with the groundwater for a short period of time, normally overnight. The bottles with the measured quantity of mixture were then placed on a shaker. The experiments were carried out for different groundwater characteristics for a definite time, and then the solids were separated from solution by filtration. The final chromate concentrations and pH were measured. The construction set up of shaken bottle experiments almost eliminated oxygen penetration from the atmosphere by the use of sealed bottles. This method enabled us to shorten the time needed to perform a large number of experiments. A large solid to liquid ratio

was maintained in these experiments so that the liquid will fill pore volume only. This corresponds to the maximum rate of reduction. It was found (35,36,37) that the primary factor in determining the rate of reaction is the available specific surface area, i.e. surface area of reactive medium per unit volume. The latter is directly proportional to the volume fraction in the solid-liquid mixture.

2.4 Column Reactor Experiment

There is a trend in the recent design of column experiment (16), which is aimed to characterize reactive media and to model some significant features of permeable reactive barriers. This is done by the use of rather small (short) columns (about 5-10 cm in length). The use of small columns in our experimental research was admissible because the effluent concentration measurement was sufficient to study the suitability of iron-pyrite mixture for chromate reduction at pH about 12. The short column experiment was necessary to carry out many experiments in parallel in order to determine the long-term performance of different types of reactive media. The column construction used in our experiments almost eliminated the oxygen penetration from the atmosphere.

Different reactive media were loosely packed in 100-ml glass columns (cross-section of 5 cm^2, height 20 cm). The columns were attached to the reservoir bottles that contained the groundwater. The pressure head was adjusted for the flow with two-velocities ranges. The first range of velocities corresponds to the larger linear velocities of the groundwater stream measured at the sites under investigation. The second range of velocities corresponds to smaller velocities, as needed for the investigation. The column effluent was collected periodically at a designated velocity. The continuous monitoring of effluent chromium concentration and its pH measurements were performed on a regular basis.

3. REACTIVE MEDIA CAPACITY AND PREDICTION OF PRB LIFETIME

3.1 Passivation of Reductive Media Surface, Reductive Capacity and Surface Area

The study of passivation kinetics (the decrease in reaction rates due to surface effects of reactive media when chromate-contaminated groundwater resides in the barrier) has to be understood, especially for the case of high pH conditions when it becomes very important.

Reactive media capacity (RMC) is a function of the linear GW velocity and the initial concentration of chromate in the sample. The smaller the velocity and the smaller the initial chromate concentration, the larger is the RMC. This regularity also agrees with the assumption that corrosion suppresses the passivation. For a time, T, if the rate of chromium accumulation is smaller than the rate of corrosion (ability to create defects in the chromium deposits), a condition may arise where the high initial reduction rate is preserved. If during the same time, T, the chromium amount accumulated is large such that corrosion may not be able to create sufficient number of defects, the reduction rate will decrease. However, at larger GW linear velocity and high initial chromate concentration, the large amount of chromate is available for reduction and passivation. Increasing the residence time is expected to suppress the passivation of the RM. Thus, the RM has to be defined by its reactive capacity dependence on GW velocity.

Also, the surface area of RM exposed to groundwater has to be taken into consideration. Agrawal and Tratnyek (35) and Matheson and Tratnyek (36) have found that the primary determinant of reduction rate is the available reactive surface area of the reactive medium. It is clear that the larger the surface area of the reactive medium, the larger the chromium amount

necessary for effecting passivation. Simple evaluation demonstrates that the passivation caused by the formation of chromium compound on the surface of reactive medium corresponds to a very short passivation time. This means that there is a mechanism which controls the surface area available for the reduction even at continuous deposition; this is believed to be corrosion. Chromium reduction in a column containing RM may be considered as a coupling of two processes, with opposite influence on the surface processes, namely: the surface passivation by the chromium deposition and surface activation due to the corrosion of RM surface. The interplay between these two processes depends primarily on the pH.

3.2 Reduction Rate and Time Dependence

For CrO_4^{2-} reduction, the elemental iron is used as a plug (short-column) filled with chromate-contaminated groundwater at pH>11. The chromium concentration is measured as a function of time. It was found that the concentration decrease is described by the exponential dependence with rate constant $K = 44\ hour^{-1}$, according to

$$n = n_i e^{(-Kt)} \qquad [3.2.1]$$

where n_i = 55 ppm is the initial concentration. The exponential dependence corresponds to the first order kinetics reaction, then

$$\ln \Delta n = -Kn\Delta t \qquad [3.2.2]$$

K is the reaction rate constant and t is the time. Its integration yields

$$\frac{dn}{n} = -Kdt \qquad [3.2.3]$$

$$\ln \frac{n}{n_i} = -Kt \qquad [3.2.4]$$

$$n = n_i e^{(-Kt)} \qquad [3.2.5]$$

The first order kinetics arises because Cr(VI) reduction is surface controlled reaction (terminology of Stumm W. "Aquatic Surface Chemistry"). As Cr(VI) ion collides with the iron particle surface, iron donates an electron to Cr(VI) and the reduction rate is proportional to the quantity of collisions of Cr(VI) ions with surface, i.e. proportional to Cr(VI) concentration. The Cr(VI) here refers to the chromate ion.

3.3 Modeling Cr(VI) Removal Within PRB at Known Filtration Velocity

At a known filtration velocity (u), through a barrier with thickness (d), Cr(VI) ion residence time is τ_{res}, is defined by:

$$\tau_{res} = \frac{d}{u} \qquad [3.3.1]$$

This residence time for the barrier is analogous to the time, T, for the batch experiments. The difference between batch experiments and Cr(VI) removal by PRB is the hydrodynamic condition and the influence of this difference with respect to reduction and passivation processes are negligible. Thus the chromium removal in batch experiments and within the PRB can be evaluated by the same set of equations using the same reaction constant K.

$$n = n_i e^{(-Kt)} \qquad [3.3.2]$$

$$n_e = n_i e^{(-Kd/u)} \qquad [3.3.3]$$

where n_i and n_e are the Cr(VI) influent and effluent concentrations.

3.4 Prediction of Chromium Distribution within a Barrier

The reactive barrier properties are considered as invariant in time, the steady distribution of chromium accumulation of the form

$$n(x) = n_i e^{(-Kx/u)} \qquad [3.4.1]$$

arises. Since there is a finite RMC with respect to chromate reduction, a layer arises within the barrier consisting of completely passivated (or consumed) RM particles. Since the chromium reduction starts at the barrier's entrance a completely passivated layer (CPL) is formed near the entrance. The thickness of the layer $l(t)$ increases with time. Since there is no further reduction possible within the CPL, the chromium concentration would not decrease along this layer, and thus would be equal to that its value before entering the barrier. Thus, the chromium distribution within the PRB can be characterized as consisting of two zones. The first zone will be having length $l(t)$ and the invariant initial concentration, n_i, and a second zone where the chromium concentration decreases from n_i to effluent concentration, n_e, the rate of first zone expansion is very small compared to the ground water velocity

$$\frac{dl}{dt} << u \qquad [3.4.2]$$

Typically, water crosses the entire length of the barrier in a period ranging from 1 to 10 days. When the CPL occupies the entire barrier, chromium leakage will become large, because the effluent concentration will be almost equal to the influent concentration. Therefore, to satisfy the long time requirement of the barrier the left-hand side of Eq. [3.4.2] has to be smaller than the right hand side by almost 1000 times.

The above prediction will enable us to formulate the chromate concentration decrease in the second zone of the barrier that is a quasi-steady state, i.e., the boundary condition relates to the mobile boundary,

$$n\big|_{x=l(t)} = n_i \qquad [3.4.3]$$

but its mobility is so low that it can be neglected. Correspondingly, the sought distribution follows Eq. [3.4.1] taking into account that $l(t)$ has to be used instead of $x = 0$ which gives:

$$n(x) = n_i \exp[-(x - l(t))K/u] \qquad [3.4.4]$$

Therefore, CPL extends very slowly, and its extension rate is determined by the chromium transport into this zone. The chromium accumulation in CPL during time, t, cannot exceed the total chromium amount entering into the barrier during this time.

We need to quantify the conditions needed for the efficient performance of the barrier, i.e., effluent flux must be small in comparison with influent flux. Let us restrict the consideration by the situation when the CPL zone occupies the main part of the barrier after a long time, i.e., when

$$[d - l(t)] << d \qquad [3.4.5]$$

In this case, the chromium amount in the second zone is very small in comparison with that in CPL and can be neglected. Keeping in mind these two conditions, the chromate conservation means that all chromium is accumulated in CPL

$$p_a n_i u t = l(t) M_{\max} \qquad [3.4.6]$$

p_a is the aquifer porosity, $M_{\max}$ is the maximum chromium amount accumulated within 1 cm^3 of RM. In this equation the units of n_i and $M_{\max}$ are grams per unit volume. Thus the ratio

$$n = \frac{n_i}{M_{\max}} \qquad [3.4.7]$$

is a dimensionless one.

It is easy to generalize Eq. [3.4.6] with account for chromium accumulated in the second zone, when the restriction in Eq. [3.4.5] is not satisfied. The condition of barrier efficient work is

$$l(T_b) <= d \qquad [3.4.8]$$

where T_b is the necessary time for efficient barrier work, or barrier effective life. Naturally, the difference between $l(T_b)$ and d has not to be very small. But it can be rather small, that is clarified with the analysis of the condition following from Eq. [3.4.3]

$$\frac{n_e}{n_i} = \exp[-(d - l(T_b))K/u] \qquad [3.4.9]$$

where $d - l(T_b)$ is the second zone thickness. The specification of the condition for K =10 hour^{-1}, d =100 cm, u =100 cm/day demonstrates that the condition

$$d - l(T_b) << d \qquad [3.4.10]$$

is satisfied due to very rapid reduction rate. The prediction of chromium concentration within the zone

$$d - l(T_b) < x < d \qquad [3.4.11]$$

needs further investigation because the distribution [3.4.9] has to be considered at first approximation based on reduction rate identification with its initial value K. In the meantime, as the CPL grows the chromate-contaminated groundwater crosses the second zone and chromium reduction and accumulation cause a decrease in the reduction rate. This decreased reduction rate constant K $[M(x,t)]$ has to be used in the equation to be more exact than the equation $dn = -Kndx$ and M value approaches to $M_{\max}$ in small vicinity of the CPL edge, i.e.

$$0 < M(x) < M_{\max} \qquad [3.4.12]$$

This means that $K(M)$ deviation from K is large near the CPL edge only. It enables to apply the method of sequent approximation. The second approximation is

$$\frac{n(x)}{n_i} = \exp[-z - (1 - e^{-z})] \qquad [3.4.13]$$

where $z = K/u(x - l(t))$. The essential difference between first (Eq. [3.4.9]) and second (Eq. [3.4.13]) approximations shows that further approximations are necessary. As a result, the zone becomes wider which calls for using a correction to the evaluation of the second zone thickness.

3.5 Evaluation of Reactive Media Capacity for Thin Plug Passivation Kinetics

The effluent concentration for a thin reactive media plug is measured as a function of time in long term experiments at the definite values of linear groundwater velocity and at its initial chromate concentration. As the effluent concentration increases till value

$$n_e(T) \sim 0.1\ n_i \qquad [3.5.1]$$

the experiment continues at smaller velocity. The total volume of liquid entered in the packed bed during time, T, is measured as $V(T_1)$. The total chromium mass accumulated in permeable barrier equals

$$m(T_1) = n_i\ V(T_1) \qquad [3.5.2]$$

It is assumed that this chromium amount is uniformly distributed within the packed bed with the volume

$$V_p = S_p \; d_p \qquad [3.5.3]$$

where S_p and d_p are the cross-sectional areas and width of packed bed, respectively. The chromium amount accumulated with 1 cm^3 of packed bed is thus:

$$C_{p1} = \frac{n_i V(T_1)}{S_p d_p} \qquad [3.5.4]$$

The measured capacity corresponds to a definite value of linear velocity and initial concentration and can be expressed by:

$$C_{p1} = C_{p1} \; (n_i, u_1) \qquad [3.5.5]$$

3.6 Critical Capacity for a PRB

The comparison of measured value of RMC, $M_{\max}$, with the barrier critical capacity, C_{bcr}, would enable us to formulate the main criteria needed for evaluating RM needed for this application. The RM can provide the needed efficiency for a successful barrier application, if its capacity to reduce chromium exceeds critical barrier capacity. If this condition is not satisfied, the RM under investigation has to be rejected and another RM with larger specific surface area or higher reactivity has to be investigated. The following equation characterizes barrier critical capacity, C_{bcr}.

$$p_a n_i u_b T_b = C_{bcr} d_b \qquad [3.6.1]$$

where u_b is the velocity within aquifer pores, p_a is the aquifer porosity.

The left-hand side of the equation yields the total chromium amount entering the barrier during a total period of time T_b. The right hand side shows the total amount of accumulated chromium in the barrier.

3.7 Prediction of Maximal Reactive Media Capacity

The determination of reactive media capacity by determining the maximum chromium amount $M_{\max}$ can be accomplished in a short duration of time compared to barrier passivation time. This is accounted by the equation

$$p_a n_i u_p T_{pcr} = M_{\max} d_p \qquad [3.7.1]$$

where d_p is the iron plug thickness, u_p is the flow velocity through the plug, T_{pcr} characterizes the time when the effluent concentration n_e becomes equal to the influent concentration n_i.

A reasonable assumption is that any cm^3 of RM within the barrier may accumulate a chromium amount C_{bcr} during time T_b almost equal to the amount $M_{\max}$ accumulated in packed bed during time T_{pcr}, because short column experiments were accomplished with the use of the groundwater of this definite contaminated site. Hence, an equation may be written

$$C_{bcr} = M_{max} \qquad [3.7.2]$$

where l.h.s. may be expressed with the use of Eq. [3.6.1] and r.h.s. with the use of Eq. [3.7.1]. This yields

$$\frac{d_b}{n_i u_b T_b} = \frac{d_p}{n_i u_p T_{pcr}} \qquad [3.7.3]$$

or

$$T_{pcr} = T_b \frac{d_p}{d_b} \cdot \frac{u_b}{u_p} \qquad [3.7.4]$$

Now it has to be taken into account that RM capacity depends on the velocity. Consequently, the condition of rigorous modeling is

$$u_p = u_b \qquad [3.7.5]$$

In our experiment the attention was paid to this condition, that simplifies condition [3.7.3]

$$T_{pcr} = T_b \frac{d_p}{d_b} \qquad [3.7.6]$$

The physical meaning of this result is very clear, namely the smaller the plug thickness, the smaller is its entire capacity and shorter time T_{pcr} after which the effluent concentration approaches the influent one. Thus, with d_p = 2 cm and d_b = 100 cm, T_{pcr} can be 50 times smaller than T_{bcr}, i.e. 2 months of plug performance would be equivalent to barrier's T_{bcr} equal to 8 years.

3.8 Number of Pore Volumes

The number of pore volumes in column experiment for reactive media should exceed that of the barrier ($NPV_{RM} >> NPV_b$) for reactive media suitability at pH equal to 12. The number of pore volumes for the reactive media is calculated by the column experiments.

$$NPV_{RM} = \frac{v_{cr}}{S_c d_c p_c} \qquad [3.8.1]$$

where NPV_{RM} is the number of pore volumes in column, S_c, d_c and p_c are cross-section area, thickness and porosity of reactive media, respectively, v_{cr} is the volume of filtrated contaminated water after which effluent concentration starts to increase.

4. RESULTS AND DISCUSSION

This section presents and discusses the results pertaining to the study of RM selection for hexavalent chromium reduction in GW, especially at high pH conditions for use in permeable reactive barriers. The GW used in the study was obtained from three sites in Hudson County, New Jersey. This section discusses the following results:

1. Iron shaken packed bed and column experiments.
2. Assessment of using iron (Fe^0) as a reactive medium at the high pH condition.
3. Assessment of using pyrite mineral as a reactive medium at the high pH condition.
4. Assessment of using iron (Fe^0)-pyrite and iron (Fe^0)-siderite mixtures as reactive media at the high pH condition.
5. Influence of hydraulic loading on the reactive capacity of iron (Fe^0).
6. Two step passivation process and total capacity evaluation.

The main objectives of this study were:

1. To evaluate the suitability of various RM for PRB applications at high pH condition.
2. To recommend application of suitable RM for long-term performance of treatment of GW.

4.1 Shaken Packed Bed Experiment

Various types of buffering systems were studied for their acid generating capacities by Desai (38). According to this study (38), silicic acid generating minerals did not exhibit adequate lowering of pH to make them suitable for use as reactive medium. This was attributed to their low dissolution rates in groundwater as discussed by Stumm (8). Phosphoric acid generating materials showed considerable solubility and pH decrease of groundwater; however, these materials were deemed impractical for use in barriers because of their fast dissolution rates. The most promising reductive media among the materials investigated by Desai (38) were H_2S-generating minerals such as iron pyrite and carbonic acid generating minerals such as siderite.

Shaken packed bed experiments were carried out with the Peerless iron materials at a residence time of 8 hours and initial chromium concentration of 16 ppm. The final chromate concentrations in the effluent were 0.05-0.1 ppm after 8 hours. The shaken packed bed experiments were accomplished for three Peerless iron materials with different particle size distribution namely: Iron #1, Iron #2, Iron #3 (Table 2.2). Iron #3 showed the lowest final chromium concentrations at residence time of 30 minutes when used with groundwater having an initial chromium concentration of 55 ppm.

The reduction rate for Iron #3 at pH = 12 is smaller than that measured at intermediate pH (up to about 9.0). Desai (38) concluded that there is a similarity in pH dependence for chromate ion reduction rate with the use of Fe^{2+} containing solutions and with the use of elemental iron (Fe^0) because the reduction rate in both cases decreases with increasing pH. In addition, the increase in iron corrosion at pH > 11 appears to be favorable for chromium reduction, as discussed below in Section 4.2.

4.2 Iron Regeneration as Reductant and Influence of Residence Time on Iron Capacity

Due to its large specific surface area, Iron #3 was used to study the reactive media capacity. The information about the deactivation kinetics was obtained by the multiple reuse of the same iron sample. After the first use, the iron was separated from the reduced groundwater. The pore volume of the same sample iron was then filled with groundwater for the second time and allowed to stand for a fixed residence time (8 hours). NPV is used as a scaling factor to extrapolate column tests to barrier field time. Increase in effluent concentration starts after the entire volume of used portions of GW equals to about 10-12 pore volumes at initial chromium concentration of 16 ppm and residence time 8 hours (Figure 4.1). The RMS is defined as the length of time (or NPV) where the RM maintains its reactivity.

The effluent concentration for first or even second reuse is very small in comparison with the initial influent concentration of 16 ppm. This indicates that the chromium amounts accumulated on the iron particle surface are almost the same for the first and second reuses.

There is a longer time available for regeneration at longer residence times. The regeneration mechanism (16) in this case appears to be related to corrosion whose role is important for chromate reduction. This was verified by varying the residence time for reuses #10 and #20 (shown by the arrows in Figure 4.1). During reuse #10 and #20, we increased the residence time that corresponded to more corrosion (regeneration) and thus resulting in lower effluent concentration.

4.3 Column Experiment

The effluent concentration for column experiment as a function of time is plotted for Iron #3 and for the initial chromium concentration of 55 ppm. The residence time at pore velocity of

0.3 cm/hour equals to 12 hours because reactive media thickness is 4 cm. At this longer residence time, the effluent concentration measured was 0.05 ppm. The increase in effluent concentration started after 10 pore volumes (Figure 4.2).

4.4 Iron Assessment as Reactive Media for pH about 12

Iron (Fe^0) as a RM has been used for chromate reduction at intermediate pH conditions (16). The estimation of iron (Fe^0) as a RM for pH about 12 was carried out in this research. When iron (Fe^0) is used as a RM, the increase of chromium concentration in the effluent at pH = 6 to 7 occur at about 80 pore volumes. The latter was the result of column investigations carried out at influent chromium concentration of 18 ppm and a pore velocity of 40m/year (16). This velocity is comparable to the velocity used in our experiments (Figure 4.2). The stability decrease at pH about 12 can be characterized as large if the difference in the initial concentrations is disregarded. However, because of the difference in the initial chromium concentrations between (16) and us, further analysis was needed as shown below.

This small difference in stability allows us to conclude that Peerless Iron #3 as a RM is not worse than the iron used in the important research for intermediate pH (16) and can also be used for further stability modeling at higher pH about 12.

The iron surface specificity does not seem to play a primary role as Sivavec and Horney (37) studied the degradation rates for chlorinated compounds with 25 types of different commercial iron sources. In addition, Agrawal and Tratnyek (35) and Matheson and Tratnyek (36) have found out that the primary determinant of degradation rates is the available specific surface area for reduction. Thus Peerless Iron #3 provides the optimal condition because its surface area essentially exceeds the typical values of iron surface area given in literature. This means that the measured stability for Iron #3 can be used to assess Fe^0 as a reactive medium at pH about 12. 10 m/year is considered in (16) to be representative of pore velocity typically observed in shallow aquifers. For velocities not very large than this, the measured number of pore volumes (10-30) is rather small compared to the 80 pore volumes at intermediate pH. These smaller values are due to the high influent chromium concentration of 55 ppm in our case. Therefore, we conclude that the iron (Fe^0) application at high pH will be limited to extreme cases of very low groundwater velocity (less than 10m/year) and to smaller chromium concentrations to achieve sufficient stability.

We conclude that a permeable reactive barrier with Iron #3 reactive medium may be suitable for treating groundwater in the case of Allied Signal site where the pore velocity is less than 10 m/year and chromium concentration is about 25 ppm. The use of iron (Fe^0) alone is not valid for the P.P.G and C.L.H. sites and therefore other reactive media are required, as will be discussed in the following sections.

4.5 Iron Siderite Mixture

Iron (Fe^0) and Siderite ($FeCO_3$) were mixed at a volumetric ratio of 50/50 and used as RM. There is a two-stage process observed in our experiment as a function of time (Figure 4.3). During the first stage, the effluent concentration values are less than the drinking water standards for chromium (0.1 ppm). The gradual increase of the effluent concentration takes place during the second stage. The chromium amount accumulated within 1 cm^3 of reactive media during first stage can be called as the RMC regarding chromium accumulation. Two long-term experiments were accomplished with iron (Fe^0)-siderite mixture (ISM) 50/50 using Iron #2/Siderite and Iron

#3/Siderite. The effluent concentration as a function of number of pore volumes is plotted in Figure 4.3.

The large influence of the velocity on NPV is seen in Figure 4.3. Iron #2/Siderite had a flow velocity of 26.5 cm/hr which is very high as compared to actual groundwater velocity while Iron #3/Siderite had a velocity of 1.9 cm/hr. The advantage of ISM 50/50 at pH = 12 is apparent even at the higher influent chromium concentration of 55 ppm. However, the siderite application can be limited because of its high solubility in water. It may occur that siderite completely dissolve in groundwater stream during time shorter than 20-30 years which makes barrier useless for longer term application with this mixture.

However, it is well known that water samples collected from some iron barriers approaches equilibrium with respect to siderite. Thus these barrier sites have to be classified into two groups namely with quasiequilibrium in the system groundwater siderite and one without quasiequilibrium. The ISM 50/50 is of primary interest in the first group of barrier sites with quasiequilibrium.

4.6 Pyrite and Siderite Solubility and its Manifestation in PRB

The most important examination concerning the pyrite and siderite relates to their solubilities in water over the long term. It is possible that these minerals may dissolve in less than 20 years, which will limit the barrier service life. Handbook data (39) for the solubility of pyrite and siderite is given as:

a) Pyrite: $0.0005 g/100 cm^3$ $(or\, 1g/2\times10^5\ cm^3)$

b) Siderite: $0.007 g/cm^3$

For the complete dissolution of one gram of pyrite, the critical volume of water v_{cr} necessary is given by

$$v_{cr} = 2\times10^5 (cm^3/g) \qquad [4.6.1]$$

Let us consider a barrier cross section perpendicular to a stream with area, S and the pyrite volume in barrier, Sdp_p where d is the width of barrier and p_p is the pyrite volume fraction. During time, T_b, the groundwater volume (uT_bS) crosses the cross-section of the barrier, i.e. this volume is available to dissolve the pyrite volume with mass $Sd\rho p_p$ where ρ is the pyrite density. Thus the ratio:

$$v_b = \frac{uT_bS}{d\rho Sp_p} = \frac{uT_b}{d\rho p_p}\left(\frac{cm^3}{g}\right) \qquad [4.6.2]$$

where u (cm/day) and T_b (day) has to be compared with v_{cr}. With d = 100 cm and T_b = 20 years, the results are given in Table 4.1:

Table 4.1: Groundwater volume per gram of RM for 20 years barrier life

$p_p \rightarrow$ u (cm/day) $\downarrow$	0.5	1.0
100	3×10^4	1.5×10^4
10	3×10^3	1.5×10^3

Small pyrite volume fraction corresponds to the reactive media soil mixture with RM volume fraction 0.2. It can be seen that pyrite solubility within the barrier in this case is not negligible. Nevertheless, this complication may not arise because GW velocity is much smaller. Siderite solubility is five times larger. Siderite application in mixture with soil at large GW velocity is not reasonable for the sites of the second type, when equilibrium is absent.

4.7 Flow Rate Influence on Accumulation of Chromium

The increase in flow rate of GW by approximately 10 times is accompanied by a decrease in reactive media capacity by 15-20 times i.e. 1 mg/cm^3 instead of 20 mg/cm^3 (Figure 4.4). This can be interpreted if we account for the competition between two processes - passivation and regeneration. In parallel with Cr(III) accumulation on the iron particle surface, which decreases a part of surface available for reduction, an opposite process takes place which regenerates the reduction ability of such surface. To illustrate these effects, the chromium reduction is accompanied with the formation of a surface compound containing Fe^{3+}. Beneath this compound, Fe^0 is present which in turn reduces Fe^{3+} to Fe^{2+}. The Fe^{2+} formation enhances the particle ability to reduce chromium because Fe^{2+} is an electron donor. Also, the simultaneous corrosion process occurring during the reaction is expected to be involved in the regeneration process.

The slower the reduction process, the stronger is the regeneration process. At higher Cr(VI) concentration, the reduction rate is higher and the rate of regeneration is lower and hence the latter cannot compete with reduction, i.e. the role of regeneration is minor in this case. At lower Cr(VI) concentration, the reduction rate is lower and the regeneration can compete with reduction i.e. the regeneration is significant.

The graphs in Figure 4.4 denote that iron/siderite mixture having flow rate of 26.5 cm/hr had rapid increase in effluent concentration at 50 pore volumes because of higher velocity than that of field conditions. Iron/siderite on the other hand with flow velocity of 1.9 cm/hr showed an increase in effluent concentration at about 550-600 pore volumes which clearly indicates that higher velocity than field groundwater velocity is not favorable for chromate removal. Also, the accumulated chromium amount per cubic cm of reactive media denotes the flow rate influence on accumulation (Figure 4.4). The chromium accumulation for iron/siderite is 2 mg/cc while that for iron/siderite is 17-18 mg/cc which clearly demonstrates the influence of flow rate on chromium accumulation.

The increase in GW velocity thus causes the decrease in the number of pore volumes. The accelerated determination of RMC by means of its measurements at velocities exceeding that of the aquifer is therefore not admissible. This is because RMC decreases very rapidly with increasing the velocity, which will cause immense underevaluation of the RMC.

4.8 Two Step Passivation Process and Total Capacity Evaluation

The two-step passivation process has to be discriminated in relation to kinetics of chromium accumulation. The first step is characterized with almost zero effluent concentration where the RMC is calculated in context of NPV. The second step of passivation takes place with continuous increase in the effluent concentration and the RMC for this step of passivation of RM is calculated by the equation:

$$C_{RM} = \frac{M_{\max}}{V(T_2)} \qquad [4.8.1]$$

where C_{RM} is RMC for the second mode of passivation with duration T_2, M_{max} is the maximal accumulated chromium and V is the volume of GW cleaned through the RM. The total capacity of RM is thus based on both first and second step of passivation kinetics.

4.9 Pyrite and Pyrite Sand Mixture

Column experiment with entire volume of pyrite equal to 25 cm^3 was conducted with initial groundwater chromium concentration of 55 ppm. The growth of effluent concentration with respect to time was observed for this reactive medium. The groundwater velocity passing through the column was maintained relatively near that of the actual groundwater velocity. The total chromium accumulation per cubic cm of reactive media was 21 mg/cc (Figure 4.5).

Pyrite and sand were mixed together at a volumetric ratio of 30/70. The total chromium accumulation per cubic cm of reactive media was 25 mg/cm^3 (Figure 4.6). The maximum capacity was calculated considering the volume of pyrite alone.

4.10 Comparison of Iron and Pyrite at pH about 12

The RMC of iron (Fe^0) alone at high pH is very low and has been found to be insufficient for use in PRB for two of the three sites. In addition, the RMC of pyrite alone were insufficient to provide the required barrier active lifetime (30 years). Therefore, a new approach for developing their mixture was investigated, as discussed below.

4.11 Iron (Fe^0)-Pyrite and Iron (Fe^0)-Pyrite-Sand Mixture

The passivation kinetics of iron (Fe^0)-pyrite mixtures (IPM) with and without aquifer material (sand) was studied. The iron (Fe^0)-pyrite mixtures were used in volumetric ratio of 50/50. The pyrite role is to decrease the pH caused by dissolution. As pyrite fraction in the mixture decreases, the useful pH decrease diminishes. Thus small amount of pyrite in the iron (Fe^0)-pyrite mixture is not favorable. On the other hand, chromium reduction occurs on iron particle surface so that small fraction of iron is not desirable.

The amount of chromium accumulated per cubic cm of reactive media for iron (Fe^0)-pyrite mixtures is shown in Figure 4.7.

In distinction from many of our experiments, this experiment was performed at low velocity similar to the velocity for 3 sites of Hudson County. This is perhaps the reason why in this experiment the maximum capacity, namely 38 mg/cm^2 is established. We shall use this value in further calculations with respect to barrier as this value is more realistic. Many other experiments with iron/pyrite underestimate real capacity because cited experiments were performed at velocities much larger than that of groundwater of 3 sites.

The iron/pyrite mixture was mixed with sand in ratio 3/7. The mean dimension of sand granules was 1.2 mm. The most interesting result is that iron pyrite capacity in this case was about 80 mg per gram of iron-pyrite mixture (Figure 4.8). It means that iron-pyrite ability to reduce and to accumulate the chromium is enhanced in presence of sand. This was earlier observed in experiments of Powell *et al.* (7) with respect to iron-sand mixture. The authors explain the mechanism of this useful phenomenon. In two other experiments with iron-pyrite-sand mixture smaller capacities were observed.

4.12 Influence of pH

The influence of pH on treatment of groundwater was studied by comparing our results with those of Blowes *et al.* (16). 80 pore volumes at intermediate pH were found by Blowes *et*

al. (16) as shown in Figure 4.9. The same regularity is inherent in our experimental data with iron (Fe^0)-pyrite mixture (IPM) as a reductant. The iron(Fe^0)-pyrite mixture gave 2000 pore volumes with effluent less than the required EPA standards (Figure 4.9).

The results of these experiments show that even at high pH conditions, the iron(Fe^0)-pyrite mixture can be used as an effective reactive medium with significant stability sufficient for long barrier lifetime.

4.15 Barrier Critical Thickness Evaluation for Sites of Hudson County, New Jersey

The reactive media capacities for iron (Fe^0), pyrite, and iron (Fe^0)-pyrite mixture with and without addition of aquifer materials (sand) are evaluated. The barrier critical thickness d_{bcr} should be:

$$d_{bcr} \leq \frac{n_i u_b T_b}{C_{RM}^{tot}} \qquad [4.15.1]$$

where n_i is the influent chromium concentration in ppm, u_b is the velocity of groundwater flowing through the barrier in cm/day, T_b is the time for barrier lifetime and C_{RM}^{tot} is the total reactive media capacity for the two modes of passivation kinetics.

5. BARRIER DESIGN AND PREVENTION OF GROUNDWATER STREAMLINING

5.1 Hydraulic Conductivities of Soil and RM

The HC of fresh iron-pyrite mixture was measured and was found to be lower than that of iron. This is because pyrite particle size is smaller than that of iron. In Table 5.1, iron-pyrite HC, K_{ip} and the range for soil HC, K_s at different points of Allied Signal site are given. Initially, the difference between K_{ip} and K_s is not very large. This conclusion changes as HC measurement was made after chromium accumulation inside the RM. With the accumulation of chromium, HC decreases 10 times. Due to this strong decrease in HC, the problem of GW streamlining around the barrier arises, and must be considered in detail for the design of a PRB.

Table 5.1: HC of site soil and iron-pyrite mixture – both fresh and after prolonged use in chromium reduction

Powder	HC (ft/day)
Site soil	1 - 19
Iron 3/pyrite mixture, fresh	2.0
Iron 3/pyrite mixture, 3 months of work	0.2

The decrease in HC can be explained by two possible mechanisms, namely: specific and nonspecific (41). The specific mechanism pertains to the accumulation of Cr as the reduction proceeds with time, as well as the deposition of other compounds such as calcium carbonate during the process. The accumulated chromium compounds occupy a large volume that decreases the dimensions of pores between particles and causes a decrease in HC. The deposition of non-soluble salts of Ca^{++} can also decrease the HC during the groundwater flow in the barrier (41). At the same deposition rate, the smaller the pores, the larger will be the HC decline by the above mechanism. The nonspecific process refers to the particle dimensions and other geometrical variables of particles inside the barrier. For example, the pyrite particles are small and can intensify the HC decline.

5.2 Barrier Specific Critical Capacity

By using the measured RM capacity, we can find out whether iron-pyrite mixture provides the barrier work for 5-20 years at pH = 12. This is done by comparing the amount of chromium which enters the barrier with the GW stream, C_{bcr} and the amount of chromium which can be reduced within the barrier. The amount C_{bcr} is proportional to chromium concentration in GW, n_i, GW stream velocity, u and time, T_b of barrier work, i.e.

$$C_{bcr} = n_i\, u\, T_b p_a \qquad [5.1]$$

C_{bcr} is the critical barrier capacity, i.e. the entire chromium amount per 1 cm^2 of barrier surface area, which crosses the barrier during time T_b and has to be reduced, p_a is the porosity of aquifer. This amount flows through a unit surface area of the barrier and has to be accumulated in a volume proportional to its thickness, d_b, i.e.

$$p_a\, n_i\, u\, T_b = c_{bcr}\, d_b \qquad [5.2]$$

This equation determines a barrier's specific critical capacity, c_{bcr} (mg/cm^3) at a given d_b value.

5.3 The Demands to the RM Capacity

The requirements for the RM capacity c_{RM}, namely the condition:

$$c_{RM} > c_{bcr} \qquad [5.3]$$

is necessary for a barrier work, where c_{bcr} relates to a definite d_b value. Eq. [5.2] is used for calculating the critical capacities for the three sites using information about the chromium concentration in GW, velocity of GW and for d_b = 1 m.

5.4 GW Streamlining Around the Barrier and Its HC

When the barrier hydraulic conductivity, K_b, is equal to the aquifer hydraulic conductivity, K_a, the GW stream is not deformed by the barrier, i.e. GW trajectories are straight lines. Any small decrease in K_b in comparison with K_a retards the GW stream and causes streamlining around the barrier. The smaller the difference between the above hydraulic conductivities, the smaller is the streamlining. In Appendix 2, it is shown (42) that the streamlining is almost negligible even if K_b is 2-3 times smaller than K_a. Thus the condition:

$$K_b > 0.3K_a \qquad [5.4]$$

is a necessary condition for a barrier design. In Fig. 5.1, there is illustration with respect to the equations given below.

$K_b = K_a$	$K_a > K_b > (0.3 - 0.5)K_a$	$K_b < 0.1K_a$
No streamlining	Streamlining is weak	Streamlining is strong

5.5 Using RM or RM/Soil Mixture at Barrier Installation

If HC of RM is much smaller than that of aquifer, a mixture of aquifer soil with RM is conventionally prepared and used as the reactive mixture for the barrier. The values of these mixtures hydraulic conductivity, K_{mix} will be between the values of HC of RM, K_{ip} and HC of aquifer, K_s, i.e.

$$K_{ip} < K_{mix} < K_s \qquad [5.5]$$

The smaller the RM volume fraction, p, the smaller the difference between K_{mix} and K_s. In our case the waste HC depository plays an additional role, as well.

5.6 GW Stream Around and Within Waste Depository and Relation to PRB Design

The three sites of Hudson County are considered as waste depositories, and this may

create a large specificity in the optimization of barrier design, and its HC condition requirements. In addition to K_s and K_{RM}, the hydraulic conductivity of waste K_w has to be taken into account. The difference between K_w and K_s complicates the GW flow field even in the absence of a barrier. The account for the regional hydraulic gradient value is not sufficient for characterizing GW flow field in this case (Appendix 3).

The GW steady flow field before a barrier installation has to be properly characterized to choose the barrier geometry and to analyze the possibility of streamlining around it. If the shape of waste depository is isometrical, i.e. its linear dimension difference in different directions is not large, it can be considered as circular. In this case, a depository can be characterized with its radius R and hydraulic conductivity, K_w. The exact mathematical description of flow field is possible in this case (Appendix 5). Three qualitative different cases can be discriminated:

$$K_w = K_s \qquad [5.6]$$

$$K_w < K_s \qquad [5.7]$$

$$K_w > K_s \qquad [5.8]$$

The water field is characterized by straight lines in the first case (Fig. 5.2a). If $K_w = 0$, i.e. a depository is not permeable for GW flow then streamlining takes place. The streamlining around a depository takes place as K_w is nonzero but small in comparison with K_s. In this case GW mainly streamlines around the depository and a small part of stream penetrates inside it. It means the flow upstream is divergent and downstream is convergent (Fig. 5.2b). In the third case, the conditions for GW flow into depository are favorable. The flow upstream of depository is convergent and downstream of it is divergent (Fig.5.2c). In Appendix 3, the flow field is quantified.

The coordinate x in the direction of regional hydraulic gradient, u_e and the circular coordinates r, θ with center at depository's center ($r = 0$) are introduced. The angles $\theta = 0$ and $\theta = \pi$ correspond to front and back poles of the depository and $\theta = \pi/2$ corresponds to its equator. The total stream of GW into a depository is obtained by integrating over its boundary in the range $0 < \theta < \pi/2$ (Appendix 3).

$$Q = \pi R^2 u \frac{2K_w}{K_w + K_s} \qquad [5.9]$$

For condition [2.3], Q can be calculated as unidirectional flow through the circular area, πR^2 as:

$$Q_{||} = \pi R^2 u \qquad [5.10]$$

The same result follows from more general equation [5.9] which simplifies at condition [5.6]. It can be seen that at condition [5.7]:

$$Q < Q_{||} \qquad [5.11]$$

and at condition [5.8]:

$$Q > Q_{||} \qquad [5.12]$$

Q growth with increasing K_w is restricted by the maximum value corresponding to:

$$K_w >> K_s \qquad [5.13]$$

This maximum value is twice larger than $Q_{||}$.

The specific GW flow field within the depository causes the necessity to specify the equation for the entire barrier capacity. It can be seen from equation [5.9] that at the same value of the regional hydraulic gradient, i.e. at the same $Q_{||}$, the entire stream through the barrier can be larger or smaller than $Q_{||}$, namely larger not more than twice and as small as K_w is small in

comparison with K_s. Thus the multiplier has to be introduced in equation for entire barrier reactive capacity [5.1]:

$$C_b = \frac{2K_w}{K_w + K_s} u_s n_i T_b \qquad [5.14]$$

The second conclusion is that the barrier needs to comprise the entire back boundary of depository, namely the arc (Fig. 5.2)

$$r = R, \qquad \frac{\pi}{2} < \theta < \pi \qquad [5.15]$$

5.7 Importance of RM Mixing with Monodisperse Fraction of Sand (Soil) for Bypassing Prevention

The mixing with coarse sand was used to provide larger HC of barrier and to prevent bypassing. Coarse sand was used rather than the aquifer material to insure that the permeability of the wall would be at least as high as that of the surrounding aquifer. The HC values of native sand and sand/iron mixture were measured as 4.37×10^{-2} cm/sec and 7.24×10^{-3} cm/sec, respectively. The larger the sand porosity, the larger will be the space available for RM to occupy pores in soil (sand). It is well known in the literature that the porosity of monodisperse powder consisting of spherical particles is 0.4 - 0.5. In polydisperse sand, porosity decreases because smaller particles occupy space between larger ones (Fig. 5.3). Thus fractionating the soil (sand) may enable us to increase RM volume fraction with the preservation of pores for water movement.

The larger the monodisperse fraction dimension, the larger will be the pores for water transport at the same RM volume fraction. However, our experiments demonstrated a difficulty which excludes the possibility of using too coarse fractionated sand. It turned out in experiments with monodisperse glass beads (1mm diameter) that RM falls down through thick pores between beads (gravitational segregation). It is well known that pores between monodisperse spherical particles are approximately 0.2 - 0.4 times of diameter. It means in this case pores of 200 μm are available which are larger than the dimensions of majority of the particles in iron/pyrite mixture. Thus, the smaller fractions of sand namely 300 - 500 micron have to be used with pores between particles smaller than iron-pyrite dimensions (50 - 100 micron).

The situation can change if the iron-pyrite mixture is aggregated because these aggregates do not fall through the small pores. The aggregate sticking to the sand surface can prevent the gravitational segregation as well.

As wet mixing enabled us to prepare sand RM mixture without gravitational segregation the measurement of the HC of the mixture K_{ip} as a function of the volume fraction of RM (iron pyrite mixture) p was accomplished. The results are given in Fig. 5.4. It is seen that at p exceeding 0.3 HC is very low, i.e. almost equal to that of RM. The strong decrease K_{ip} occurs in p values 0.2-0.3. Volume fraction 0.25 in combination with large sand grain about 1.5-2 mm may be recommended. Although the mixture HC is 3-5 times smaller than that of sand it is larger than that of an aquifer because of very large HC of the coarse sand. Naturally, if the aquifer consists of the coarse sand this conclusion is not valid.

This was confirmed in our experiments with wet mixing of sand with iron pyrite mixture. It was found that there is no gravitational segregation of small pyrite particles with respect to much larger sand particles (about 1.2 mm). Wet iron pyrite mixture sticks to sand surface. One concludes that the wet mixing technology may be proposed for the preparation of iron pyrite

sand mixture for the barrier installation. As the sand particles in this mixture may be rather large (1 mm or even 2 mm) the mixing with the sand will prevent bypassing.

5.8 Method of HC Ratio Measurement

Although the problem with bypassing is eliminated due to wet mixing with coarse sand HC ratio significance preserves because of its influence on the critical barrier capacity according to Eq. [5.14]. The information about soil HC and waste depository HC is necessary as a function of depth because of HC's dependence on depth. This is a routine measurement for soil. Since the depository is toxic, these measurements are difficult and direct K_w measurement should be avoided. It is sufficient to measure convergent or divergent GW velocity distribution upstream of depository. The convergency corresponds to HC ratio smaller than 1 and the divergency corresponds to HC ratio larger than 1.

5.9 Possibility of HC Decline Prevention for RM/Sand Mixture at Optimal Mixing Regime

The possibility of the large sand particle use in wet mixing process eliminates the possibility of pore clogging due to the precipitation because the pores are rather large. However, the energy consumption at wet mixing is much larger than at dry mixing. The energy consumption problem may arise if a large amount of mixture is necessary for a barrier installation. Hence, dry mixing may be preferred if the aquifer and depository conductivities are rather small. The problem of precipitation discussed below arises in this case.

Let us consider an RM/monodisperse sand (soil) mixture prepared in two very different mixing regimes:

a) Regime of ideal mixing (Fig. 5.5a),

b) Regime of weak mixing (Fig. 5.5b).

If RM particles are distributed uniformly between sand particles then it is called ideal mixing. Perhaps the ideal mixing cannot be realized so we will consider real mixing which is close to the ideal one.

In weak mixing (partially segregated), small portions of RM particles are preserved between sand particles in distinction from ideal mixing. When the difference in mean dimensions of RM and sand is three or more times, the number of RM particles exceeds the number of pores between sand particles (this number is 27 or more times larger than the sand particle numbers). If the number of RM particles exceeds the pore number and RM particles are uniformly distributed within the sand particles then all or most of the pores are filled with RM particles at almost ideal mixing.

For the ideal mixing, the deposit growth on RM particle inside a pore decreases the free space in the pore. As majority of pores are filled with RM and as HC of any pore declines due to either chromium compound formation or Ca++ salt deposition, the entire HC of RM/sand mixture decreases approximately as much as local HC decrease. This decrease in HC may be negligible in the case of weak mixing because there is only a local HC decrease inside RM particle portion. If the local HC of RM particle portion is reduced by 1000 times, it will only cause 10% decrease in the HC of RM/sand mixture. This is because the high HC of sand is preserved and the sand occupies 80 - 90% of RM/sand mixture space at RM p_{opt} of 0.1 - 0.2. In other words, there is local HC decrease inside isolated RM particle portions, which occupy 10-20% of the space of RM/sand mixture, that cannot cause the decrease of mixture entire HC, exceeding 0.1 - 0.2 according to reliable theory of transport phenomena in disperse systems (43) (Appendix 4). There will be a retardation in the transport step of chromium reduction process in

the case of weak mixing. However, this retardation can be neglected at proper weak mixing (Appendix 4). It is not easy to exclude that optimized weak mixing can prevent a large HC reduction even at $p_{opt} > 0.2$.

5.10 Layered Mixing of RM with Sand (Soil)

The perspective of p_{opt} increase at optimized weak mixing is of great technological importance. However, this optimization will be very difficult because its modeling and control are not easy. The experimental results obtained for mixing in a small volume cannot be used for the prediction of large scale mixing. The mixing results control means the determination of RMPP of their dimensions which is a time consuming process. Unfortunately, a simpler procedure of the mixing results evaluation by means of HC measurements is even more difficult than RMPP distribution characterization. This is because HC is of interest not for initial moment but after the chromium or calcium deposit formation and that takes many months. This is the advantage of RMPP determination since its measurement soon after the mixing enables us to predict the long term HC decrease. Thus, the weak mixing technology will not be more difficult than conventional technology of sand RM mixing for barrier. Moreover, the energy consumption will be decreased because weak mixing takes less time than ideal mixing. However, the investigations for optimized regime determination will be very time consuming and expensive.

A simpler approach to prevent large HC decrease at chromium reduction deserves attention. We introduce a qualitative different approach called layered mixing. Instead of mixing RM and sand, horizontal layers of RM and sand particles are formed and arranged as a periodical structure (Fig. 5.6). Since the high HC condition is preserved within sand layers, the decrease in HC will only take place within the RM layers. The HC of this layered system is given as:

$$K_l = \frac{d_s K_s + d_{RM} K_{RM}}{d_s + d_{RM}} > \frac{d_s}{d_s + d_{RM}} K_s \qquad [5.16]$$

This equation is of large technological importance if K_l can be 0.5 K_s or larger. Two advantages can be achieved with this layered structure. First, the condition [5.4] is satisfied, i.e. bypassing can be avoided. Second, the larger volume fraction of RM needed to provide the required reactive capacity of a barrier with reasonable thickness can be easily satisfied.

The property of powder to flow along narrow vertical capillary under gravitational influence can be used for producing a layered powder structure. A vertical capillary is opened from both sides. The capillary's upper opening is used for its continuous feeding with powder. The flow along capillary is accompanied with the formation of narrow vertical stream. The deposit formation due to this stream can be controlled by the velocity of the capillary horizontal movement. The larger the velocity, the thinner will be the layer. A slit capillary can be used instead of cylindrical one. It will provide a slit like vertical powder stream. Its horizontal dimension can be as long as necessary, for example 1-3 meters. This enables us to form layer structure on a large surface (10 m^2 or more). By using two slit capillary, two layers namely a sand layer and an RM layer can be formed together. If sand capillary is first in the direction of capillary's horizontal movement a sand layer is formed and then an RM layer is formed over the sand layer.

A simple mechanical device for layered powder 2-component system formation can be designed for its application in a trench for barrier. The growth of layered system height within the trench is accompanied with its weight increase and the system compaction. Some distortion of layered system during compaction is possible. The layers are bent or even some cracks are developed. However, a mixing process is necessary to destroy layered system completely. But

there is no mixing process within the barrier so the partial distortion of layered system will not cause a serious change in its high HC. Another possibility is the industrial production of layered system as blocks and incorporation of blocks into the trench. In layered system, GW flows mainly along the sand layer and chromium ions penetrate from this flow into RM layer due to molecular diffusion. The diffusion is a slow process. The exact theory of diffusion of chromium into RM layer is under preparation. According to preliminary evaluation, the necessary layer thickness is between 5 mm and 2 cm.

5.11 Evaluation of Barrier Critical Thickness

This evaluation is done with the use of RM sand mixture with iron pyrite 50/50 mixture as RM. The soil RM/sand volume ratio is taken rather small, namely 0.2, because there is a large uncertainty with respect to soil HC caused with its large heterogeneity, i.e. large difference for different points of a site. According to our measurement RM (iron/pyrite) capacity in mixture with sand is about 80 mg per 1 cm^3 of RM. It may be easily recalculated per 1 cm of RM sand mixture

$C_{mix} \sim 80x0.2 = 16\ mg/cm^3$ [5.17]

Usually the calculations are made for a barrier thickness of 1 meter. A larger thickness can be used as well. The larger thickness enables us to use larger amount of RM. On the other hand, very large thickness is not admissible. Thus, the concept of barrier critical thickness d_{bcr} is valuable. d_{bcr} is the minimal barrier thickness which provides reduction for 30 years. It means that 1 cm^3 of barrier will accumulate the maximum chromium amount. Thus, C_{RM} is substituted into equation [5.2] to yield:

$$d_{bcr} = \frac{p_a n_1 u T_b}{C_{RM}} \qquad [5.18]$$

In the case of barrier installation using RM soil mixture, its capacity C_{mix} has to be substituted into equation [5.18]

$$d_{bcr} = \frac{p_a n_1 u T_b}{C_{mix}} \qquad [5.19]$$

The specification of equation [5.19] using equation [5.14] yields:

$$d_{bcr} = \frac{p_o n_1 u T_b}{C_{mix}} \cdot \frac{2K_w}{K_w + K_s} \qquad [5.20]$$

For condition [5.8] the second multiplier value approaches to 2. It means the larger HC of waste depository can cause the necessity to increase the barrier thickness twice. The value 2 for the multiplier is a useful approximation as K_s is small as compared to K_w and can be omitted in the denominator. For condition [5.7] a large decrease in the barrier thickness is possible because almost linear decrease of GW flow rate through the barrier takes place with decreasing HC of waste depository. For the preliminary evaluation of the barrier thickness, the second multiplier in equation [5.20] is replaced with 1 because the information about the ratio K_w/K_s is not available. For the three sites, the values for chromium concentration in GW and GW velocities are taken from Table 2 and are substituted into equation [5.20]. The value of 16 mg/cm^3 is taken for C_{mix}. The porosity 0.3 is taken for C.L.H. and 0.4 for P.P.G. Two columns correspond to lower and larger HC of depository. The line d_b yields the results of calculation according to Eq. [5.20]. The calculations are made for 30 years. The line $\overline{d}_b$ yields the recommended thickness for barrier.

Table 5.2.

	C.L.H.				Allied Signal		P.P.G.	
Concentration (ppm)	55				25		16	
GW velocity	0.17 f/d*		0.84 f/d		13 f/y	35 f/y**	0.5 f/d	
GW velocity (cm/day)	5.2		26		1.1	3.0	15.2	
$2K_w/(K_w+K_s)$	1	2	1	2	2	2	1	2
d_b	0.6	1.2	3	6	0.15	0.5	0.6	1.2
$\overline{d}_b$	1	1	1.8	3.6	1	1	1	1

*f/d-foot per day; **f/y-foot per year

As backhoe excavation provides the trench width 1 m, smaller numbers with small difference from 1 are replaced with 1. In cases when the calculated value is larger it is possible because the mean value of concentration is smaller than the maximum value used in calculation. Rather large thickness in C.L.H. case with the use of maximal velocity may be decreased at least twice, 1.8 and 3.6, because the mean velocity may be taken instead of maximum. According to private information of Dr. Harris the real concentration has to be smaller than 55 ppm, because this value was one among many concentrations measured in different points of this site.

6. DIFFERENT VARIANTS OF BARRIER HYDROLOGICAL DESIGN

6.1 Advantage of Continuous Barrier Configuration and Disadvantage of Funnel and Gate System Regarding Chromium Reduction at High pH

In this investigation, a modest RM capacity at high pH is established and therefore, the continuous barrier configuration has advantage over the funnel and gate system. The critical barrier capacity was evaluated above regarding continuous configuration. As it can be seen from Table 5.2, a rather large barrier thickness is necessary for C.L.H. to increase RM amount inside a barrier.

Regarding funnel and gate configuration (44), the evaluated barrier thickness within gate has to be increased *g* times, where *g* is the ratio of the gate length to the gate width. This is caused by the necessity to preserve RM amount within the barrier, i.e. to preserve the entire volume of a barrier at the transition from the continuous configuration to funnel and gate configuration. Thus, if the length of RM layer decreases g times, its thickness has to be increased g times. Also, the velocity through the gate has to be g times larger. This is possible with the increasing HC within the gate. Meanwhile, RM and even RM/soil mixture usually have smaller HC. Thus, the problem of providing a large capacity and high HC at the same time becomes more difficult with the use of funnel and gate configuration.

The advantage of a funnel-and-gate system over an *in-situ* reaction curtain is that a smaller reactive barrier can be used for treating a given plume which may lead to lower cost. If the barrier requires periodic replacement, it will be easier to accomplish if this barrier is enclosed in a relatively small gate than if it is spread across a large extent of aquifer, as in the case of *in-situ* reaction curtain (44). As a rather large amount of RM is necessary to accumulate chromium, the reactive barrier enclosed in a relatively small gate becomes impossible. This is even more difficult as RM has to be mixed with a large amount of soil or sand (5 – 10 times).

6.2 Variable Thickness of Barrier in the Continuous Configuration

In the absence of a barrier, the radial velocity changes very strongly along the back

boundary of waste depository with its maximum value at back pole and its zero value near the equator. This distribution is preserved with a barrier installation because the bypassing has to be avoided. This means the contaminated GW stream through barrier changes along its length. Correspondingly, the amount of chromium accumulated within barrier is maximal near the back pole of depository and decreases as it approaches the equator. As the barrier thickness has to be proportional to the chromium flux through it and the latter changes along it, the variable thickness of barrier is reasonable (Fig. 6.1). As the maximum barrier thickness necessary in the vicinity of its back pole is very large, a decrease in installation expenses can be achieved by decreasing the barrier thickness as it approaches the equator.

6.3 Barrier Configuration Supplemented with Upstream Cutoff Walls

According to Table 5.2, a very large barrier thickness will be required in the case of C.L.H. and the use of *in-situ* reaction curtain would be impracticable. In this situation the idea formulated in (44) deserves an attention: "A contaminant source zone can be completely surrounded by cutoff walls except for a gap that is left on the down gradient side. The upstream wall deflects most of the groundwater around the contaminant source zone. Water that infiltrates into the enclosure or flows through the cutoff walls into the cell exits through the gap, where an *in-situ* reactor remediates the groundwater. This configuration minimizes the amount of water that flows through the contaminant source zone and hence the amount of contaminated ground water that must be treated. It also maximizes the retention time in the gate which leads to more complete treatment (44)" (Fig.6.2).

7. QUALITY ASSURANCE

There are 3 sources of errors in predicting a PRB thickness sufficient for chromium accumulation during 30 years. These are as follows:

7.1 Errors in experimental determination of RM capacity

The amount of chromium accumulated in a thin plug of RM is determined by measuring the difference between influent and effluent concentrations. The error in measurement of a rather large influent concentration (16-55 ppm) is less than 0.5%.

In the most important long-term experiments the final effluent concentration was 10-30 ppm. The errors in determination of the influent and effluent concentrations have to be summed, that yields the error about 1% in evaluation of RM capacity. The error in determination of the effluent concentration increases when it is low. At its value 1 to 3 ppm the error increases to 10%. However, this does not cause a large error in RM capacity determination because the difference between the influent and effluent concentrations is determined mainly with high influent concentration, when the effluent concentration is low. For example, the absolute error in measurement of the effluent concentration about 5 ppm is 0.3 ppm when the relative error is 10%. But 0.3 ppm causes the error less than 1% in determining the difference between the influent concentration 5 ppm and effluent one (3 ± 0.3) ppm.

Mainly there were 2-3 parallel long term investigations with the same RM and the same velocity. The difference between these parallel measurements of RM capacity was mostly less than 3% but larger than according to evaluation given above. This was caused by the strong influence of velocity on the capacity and the velocity fluctuations during experiment. These fluctuations were caused with the deposit formation within valve whose cross-section was 1000

times smaller than that of packed bed columns. Although the needed velocity was periodically reestablished it was impossible to introduce this correction immediately, because the experiment proceeded 24 hours per day.

At the necessity of a large amount of long term experiments, mainly iron/pyrite and iron/siderite mixtures, iron/pyrite/sand and iron/siderite/sand mixtures, it was impossible to arrange more than 2 parallel experiments with their duration about 10-12 months. Thus the main results, namely RM capacity about 80 in iron/pyrite mixture with sand was obtained in 2 experiments. RM/sand mixture ratio was 3/7 and 1/20 in these experiments and both experiments gave the capacity about 80 mg per 1 gram of iron pyrite mixture.

There were a large number of experiments with short duration, namely about 3 months. The slope characterizing the effluent concentration vs. time was rather low and stable in time. This was used for extrapolation. The capacity about 80 mg/cm^3 was calculated by means of extrapolation as well.

7.2 Errors in the modeling of reduction dynamics within PRB and correspondingly errors in the prediction of its thickness

Modeling of barrier critical capacity is based on the assumption that any sub-layer of small thickness about 3-5 cm accumulates the same chromium amount as RM capacity (that is similar to the thin packed bed thickness in the experimental column) within first layer in the 3 layer model of chromium accumulation dynamics after a rather long time about 1 year.

This enables to predict the necessary PRB thickness by means of dividing the entire amount of chromium crossing PRB during 30 years on RM capacity. Although this assumption follows from exact quantitative physico-chemical analysis, it was confirmed by special experiments. In these experiments iron was used as RM because its capacity is 30 times lower than that of iron/pyrite mixture. But even at small iron capacity, this experiment took about half year.

Two columns were filled with the same iron. The iron layer thickness in column 1 was 4 cm and 20 cm in column 2. At the same velocity, the effluent concentration growth started after shorter time in column 1 and after longer time in column 2. This breakthrough time in case of column 2 was about 5 times longer than in case of column 1. Correspondingly, the chromium amount accumulated within column 2 was 5 times larger than that accumulated within column 1. This experiment confirms that it was sufficient to measure the amount of chromium accumulated during a rather short time (about 1 month) at small packed bed thickness to predict the amount of chromium, which will be accumulated in longer packed bed and to predict its lifetime.

The identification of the first layer thickness with the barrier thickness causes an error, which may be evaluated as the ratio of the thickness of the third layer to the barrier thickness. This thickness at the end of the barrier life has to be accounted for. This thickness of the clean third layer has to be sufficient to provide a small effluent concentration. Our experiment with small column shows that this thickness may be very small in comparison with a PRB thickness. It is much less than 4 cm, because 4 cm provided chromium removal. At the end of our long term experiment, the third layer thinner than 1 cm provided the chromium removal.

Such a small thickness of third layer sufficient for chromium removal is due to a very low velocity in PRB and correspondingly in our experiments with low velocity. Thus the identification of the first layer thickness with PRB thickness (about 100 cm) causes the error about 1-2%.

7.3 Errors caused by the uncertainty of information

These errors are caused by the uncertainty of information about chromium flux through the designed barrier especially with respect to C.L.H. site; for the other 2 sites the entire amount of chromium is much lower and errors are minimized, i.e., for the P.P.G. and Allied Signal sites, even large error in estimating GW velocity and concentration about 50% may not change the conclusion about the barrier thickness about 1 meter as sufficient for 30 years.

Among 3 sources of errors the first and second sources may be neglected because the errors caused with them, namely 1-3%, are an order of magnitude smaller than errors caused with uncertainty in GW stream characterization, which is important in C.L.H. case. Only the absence of information about divergent/convergent flow for waste depository causes the variation in the necessary PRB thickness 100%. In addition the seasonal variation in GW velocity and chromium concentration and a large heterogeneity of the aquifer which causes large difference in velocity measured in different points may be accounted in future to specify the recommendation for C.L.H case.

8. CONCLUSIONS AND RECOMMENDATIONS FOR FUTURE RESEARCH

At high pH about 11-12, iron pyrite mixture mixed with coarse sand provides in parallel the sufficient RM capacity and rather large HC which eliminates bypassing. The method for predicting the necessary PRB thickness is confirmed by both theory and experiment. As the step of the experimental research and the modeling is accomplished and as results are promising the next step includes the perfection of GW stream characterization for C.L.H. and the pilot investigations.

9. RECOMMENDATIONS AND APPLICATION AND USE BY NJDEP

1. At high pH about 11-12 iron-pyrite mixture is recommended as the reactive media (RM).
2. The mixture of iron pyrite and a coarse sand (1 to 2 mm) is recommended to provide in parallel rather large RM capacity and sufficiently high hydraulic conductivity (HC). As HC of this mixture exceeds that of the aquifer for the 3 sites of Hudson County bypassing will be eliminated. The RM/sand ratio should not exceed 1/5 because with higher RM content HC decreases very strongly.
3. The dry mixing of RM with coarse sand is not recommended because of the gravitational segregation (smaller pyrite particles fall through the large pores between large sand granules). As a result RM concentration may decrease very much within top part of the barrier. However, this phenomena, needs to be confirmed at pilot investigation with large mixed RM sand height.
4. Wet mixing is recommended to avoid the gravitational segregation. The energy consumption for wet mixing has to be evaluated for large scale mixing.
5. Barrier thickness of 1 meter may be sufficient to provide the necessary capacity for 30 years of barrier life in case of Allied Signal and P.P.G.
6. In case of C.L.H., barrier thickness in the range 1.8-3.6 may be recommended. For the further specification of the barrier thickness, the GW flow within the waste depository and outside has to be investigated in detail because of the phenomenon of convergent/divergent flow caused by HC difference between the depository and the surrounding media. Equations are derived which predict the convergent/divergent flow

influence on the barrier critical capacity. The barrier thickness for C.L.H. may be further specified with the use of these equations after the information about convergent/divergent flow is compiled. The detailed information about seasonal variation in GW velocity and chromium concentration is also necessary to make estimation of critical barrier capacity and thickness.

REFERENCES

1. Blowes D. W., and Ptacek C. J., "System for Treating Contaminated Groundwater" United States Patent # *5,362,394*, 1994.
2. Blowes D. W., and Ptacek C. J., "System for Treating Contaminated Groundwater" United States Patent # *5,514,279*, 1996.
3. Kirk R. E., and Othmer D. F., Encyl. Of Chem. Tech., 4th Edition, John Wiley and Sons, New York, NY, USA, 1992, Vol. 6, 229, 284.
4. Nriagu J. O., and Neiboer E., Chromium in the Natural and Human Environments, John Wiley and Sons, New York, NY, 1988.
5. Zachara J. M., Girvin D. C., Schmidt R. L., and Resch C. T., Chromate Adsorption on Amorphous Iron Oxyhyroxide in the Presence of Major Groundwater Ions, Environ. Sci. Technol., 1987, 21 (6), 589-594.
6. Gould J. P., The Kinetics of Hexavalent Chromium Reduction by Metallic Iron, Water Research, 1982, 16 (6), 871-877.
7. Powell R. M., Puls R. W., Hightower S. K., and Sabatini D. A., Coupled Iron Corrosion and Chromate Reduction: Mechanisms for Subsurface Remediation, Environ. Sci. Technol., 1995, 29 (8), 1913-1922.
8. Stumm W., Morgan J. J., Aquatic Chemistry, John Wiley and Sons, New York, NY, 1981.
9. Gillham R. W., and O' Hannesin S. F., Metal-Catalysed Abiotic Degradation of Halogenated Organic Compounds, "Modern Trends in Hydrogeology", International Association of Hydrogeologists (IAH), 1992, Hamilton, Ontario, Canada, 94-103.
10. Gillham R. W., and O' Hannesin S. F., Enhanced Degradation of Halogenated Aliphatics by Zero-Valent Iron, Ground Water, 1994, 32 (6), 958-967.
11. Skoog D. A., and West D. M., Fundamentals of Analytical Chemistry, Saunders College Publishing, New York, NY, 1983, 859.
12. Bowers A. S., Ortiz C. A., and Cardozo R. J., Iron Process for Treatment of Cr (VI) Wastewaters, Metal Finishing, 1986, 11, 37-41.
13. Anderson L. D., Kent D. B., and Davis J. A., Batch Experiments Characterizing the Reduction of Cr (VI) using Suboxic Material from a Mildly Reducing Sand and Gravel Aquifer, Environ. Sci. Technol., 1994, 28 (1), 178-185.
14. Stollenwork K. G., and Grove D. B., J. Environ. Qual., 1985, 14, 396-399.
15. Shokes T. E., and Moller G., Removal of Dissolved Heavy Metals from Acid Rock Drainage using Iron Metal, Environ. Sci. Technol., 1999, 33 (2), 282-287.
16. Blowes D. W., Ptacek C. J., and Jambor J. L., In-Situ Remediation of Cr (VI)-Contaminated Groundwater using Permeable Reactive Walls: Laboratory Studies, Environ. Sci. Technol., 1997, 31 (12), 3348-3357.
17. Wilson E. K., Zero-Valent Metals Provide Possible Solution to Groundwater Problems, Chemical & Engineering News, 1995, 73 (27), 19-23.

18. Bennet T. A., Blowes D. W., Puls R. W., Gillham R. W., Hanton-Fong C. J., Ptacek C. J., O'Hannesin S. F., and Vogan J. L., Design and Installation of an In Situ Porous Reactive Wall for Treatment of Cr (VI) and Trichloroethylene in Groundwater, Preprint Extended Abstracts from 213th ACS National Meeting, Anaheim, CA, 37 (1), 243-245.
19. Gillham R. W., Blowes D. W., Ptacek C. J., and O'Hannesin S. F., Use of Zero-Valent Metals for In-Situ Remediation of Contaminated Groundwater, In: In-Situ Remediation: Scientific Basis for Current and Future Technologies, Gee G. W. and Wing N. R. (Eds.), 1994, Battelle Pacific Northwest Laboratories, Pasco, WA, Part 2, 913-930.
20. Higgins T. E., and Marshall B. R., Combined Treatment of Hexavalent Chromium with other Heavy Metals at Alkaline pH, Proceedings of 17th Mid-Atlantic Industrial Waste Conference Toxic and Hazardous Wastes, 1985.
21. Eary L. E., and Rai D., Kinetics of Chromate Reduction by Ferrous Irons Derived from Hematite and Biotite at 25°C, Am. J. Sci., 1989, 22, 180-213.
22. Toyoaki Aoki, and Makato Munemori, Reduction of Cr (VI) by Fe (II) Hydroxide in Alkaline Solution, Bull. Chem. J., 1982, 55, 730-732.
23. Burris D. R., Campbell T. J., and Manoranjan V. S., Sorption of Trichloroethylene and Tetrachloroethylene in a Batch Reactive Metallic Iron-Water System, Environ. Sci. Technol., 1995, 29 (11), 2850-2855.
24. Hosler R. A., McCutcheon S. C., and Wolfe N. L., Mass Transfer Effects on the Dehalogenation of Trichloroethene by Iron/Pyrite Mixtures, Preprint Extended Abstracts from 209th ACS National Meeting, Anaheim, CA, 35 (1), 778-779.
25. Ullman F., Encyl. Of Ind. Chem., 5th Edition VCH Publishers, Florida, USA, 1985, A-7, 72-76
26. Kirk R. E., and Othmer D. F., Encyl. Of Chem. Tech., 4th Edition, John Wiley and Sons, New York, NY, USA, 1992, Vol. 6, 228-239.
27. McKetta J. J., Encyl. Of Chem. Processing and Design, Marcel Dekker Inc., New York, NY, USA, 1979, Vol. 8, 308.
28. Barlett R. J., and James B. R., " Behavior of Chromium in Soils: III Oxidation". J. Environ. Qual., 1979, Vol. 8 (1), 31-34.
29. Kirk R. E., and Othmer D. F., Encyl. Of Chem. Tech., 4th Edition, John Wiley and Sons, New York, NY, USA, 1992, Vol. 6, 288.
30. Kirk R. E., and Othmer D. F., Encyl. Of Chem. Tech., 4th Edition, John Wiley and Sons, New York, NY, USA, 1992, Vol. 6, 284.
31. Gavaskar A. R., Gupta N., Sass B. M., Janosy R. J., O'Sullivan D., Permeable Barriers for Groundwater Remediation: Design, Construction, and Monitoring, Battelle Press, Columbus, OH, 1998.
32. US-EPA method # 7000, SW-846, 3rd Edition, 1986.
33. US-EPA method # 7196, SW-846, 3rd Edition, 1986.
34. US-EPA method # 7196-A, SW-846, 3rd Edition, 1986.
35. Agrawal A., and Tratnyek P. G., Abiotic Remediation of Nitro-Aromatic Groundwater Contaminants by Zero-Valent Iron, 1996, Preprint Extended Abstracts from 207th ACS National Meeting, San Diego, CA, 34 (1), 492-494.
36. Matheson L. J., and Tratnyek P.G., Reductive Dehalogenation of Chlorinated Methanes by Iron Metal, Environ. Sci. Technol., 1994, 28 (12), 2045-2053.

37. Sivavec T. M., and Horney D. P., Reductive Dechlorination of Chlorinated Ethenes by Iron Metal, 1995, Preprint Extended Abstracts from 209th ACS National Meeting, Anaheim, CA, 35 (1), 695-698.
38. Desai S. Hemant, Study of Reactive Media for Chromium Removal from Groundwater by Permeable Barriers, Masters Thesis, May 1999.
39. Handbook of Chemistry and Physics, CRC Publication, 78th Edition, 1997-1998.
40. Powell, R. M., Puls, R. W., Hightower, S. K. and Sabatini, D. D., *Environ. Sci. Technol.*, 29, (1995), 1913-1922.
41. O'Hannesin, S. F. and Gillham, R. W., *Gr Water Monit. Remed. 1*, 1998, 164-170.
42. Starr, R. C. and Cherry, J. A., *Ground Water*, 12(30, 1994, 465-476.
43. Ijoor, G. C., "Modeling of a Permeable Reactive Barrier," *Masters Thesis*, New Jersey Institute of Technology, Newark, NJ, 1999.
44. Dukhin, S. S. and Shilov, V. N., *Dielectric Phenomena and the Double Layer in Disperse Systems and Polyelectrolytes*, John Wiley, New York, 1974, Chapter 2, paragraph 1 (Dielectric Phenomena in a Mixture of Components with Different Conductivities) and Chapter 6, paragraph 2 (Principle of Generalized Conductivities).

Figures

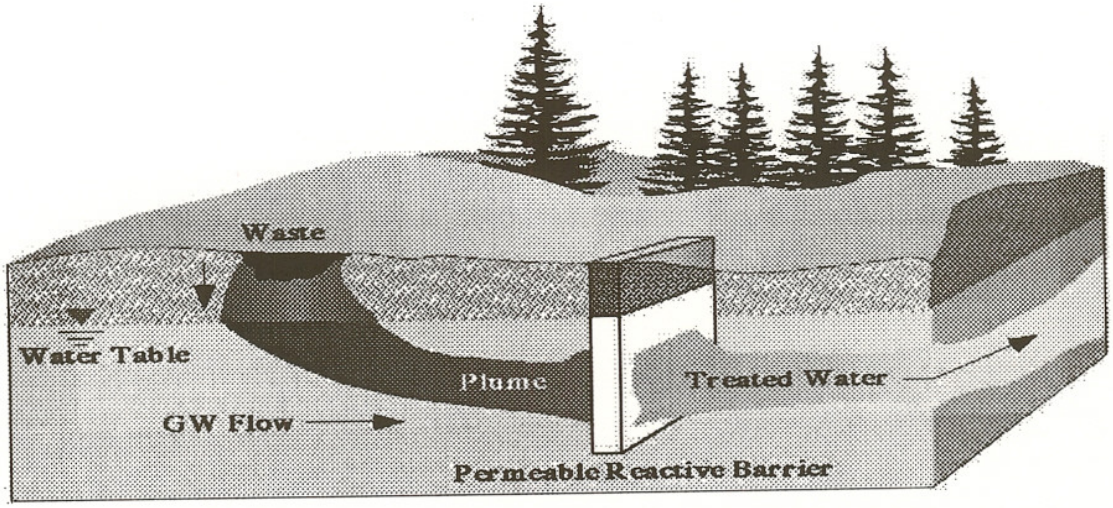

Figure 1.1: Permeable reactive barrier

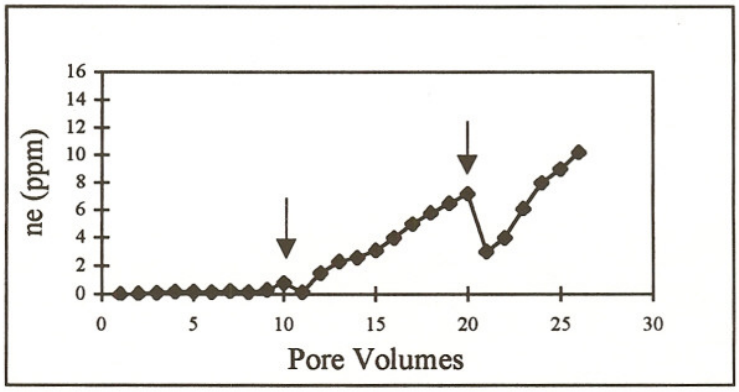

Figure 4.1: Result of shaken packed bed experiment (arrows indicate the increase in residence time for reuse # 10 and # 20)

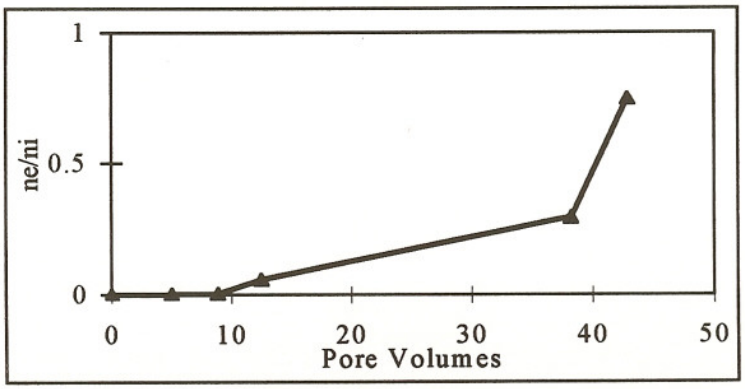

Figure 4.2: Growth of effluent concentration for Iron # 3

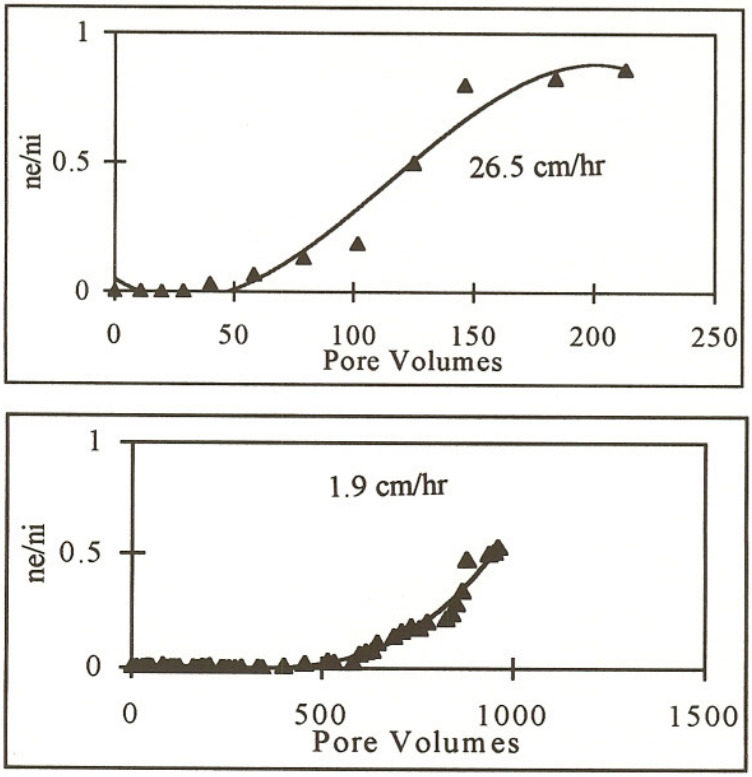

Figure 4.3: Results of column experiments with ISM volumetric ratio 50/50

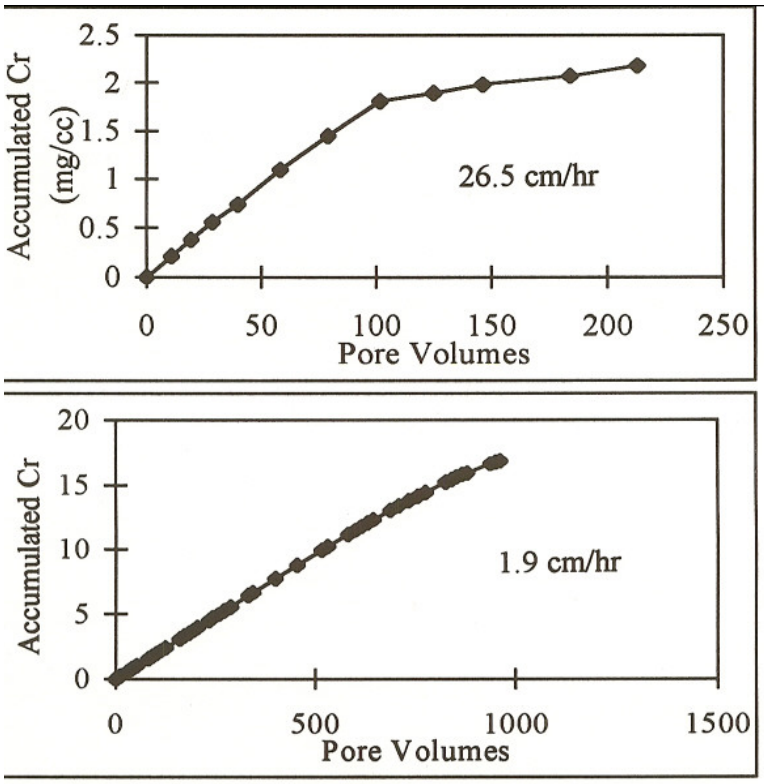

Figure 4.4: Flow rate influence on chromium accumulation

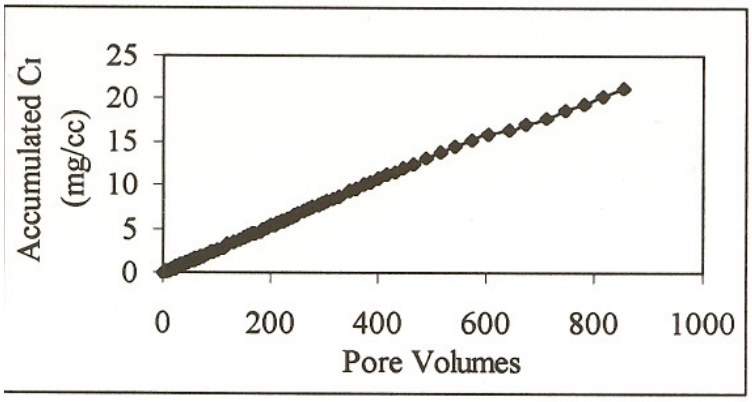

Figure 4.5: Accumulated chromium for pyrite experiment

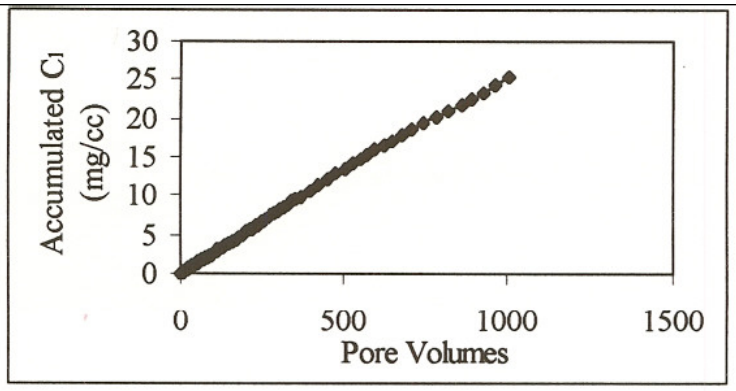

Figure 4.6: Accumulated chromium for pyrite sand experiment

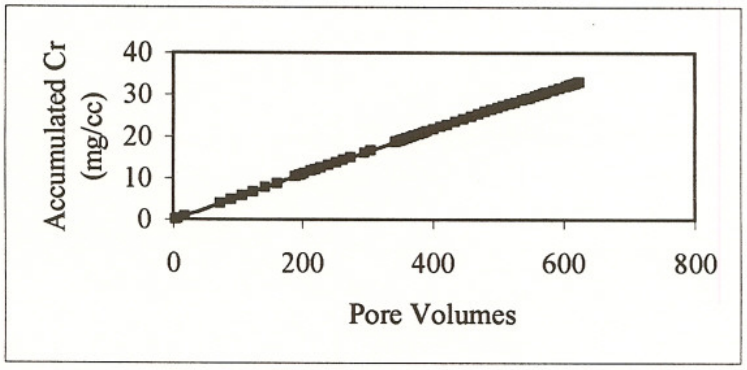

igure 4.7: Accumulated chromium for iron (Fe^0)-pyrite-sand experiment

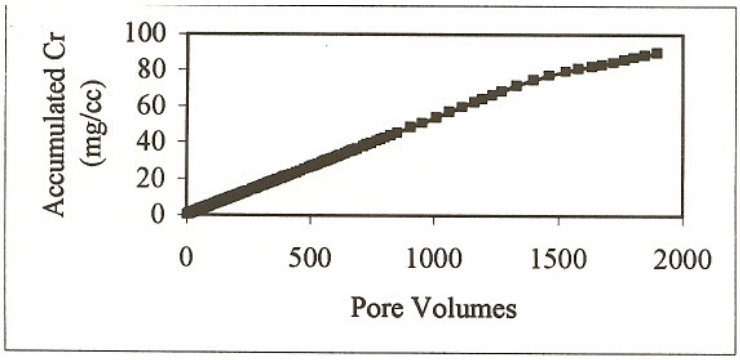

Figure 4.8: Accumulated chromium for iron (Fe^0)-pyrite experiment

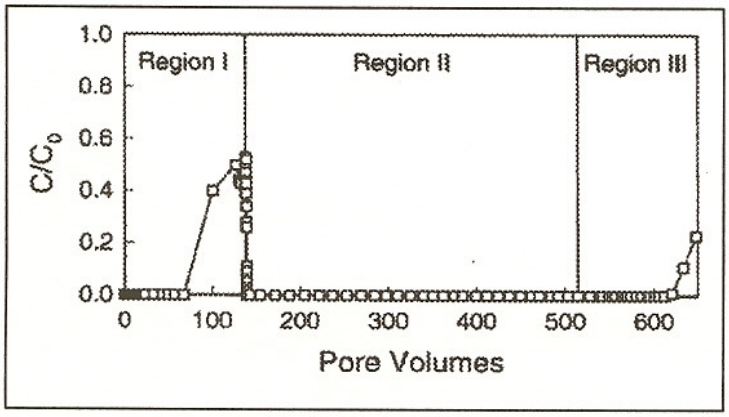

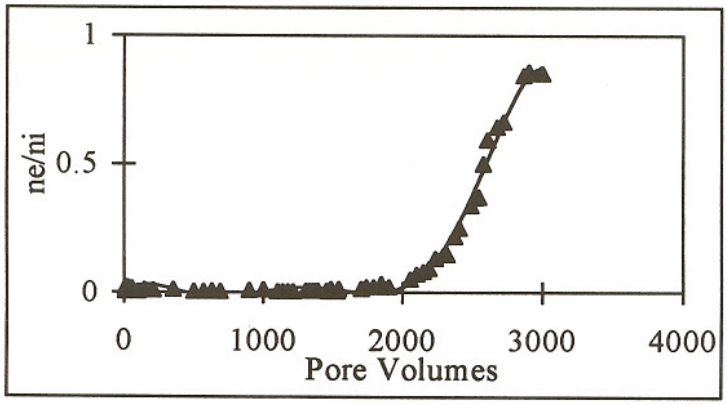

Figure 4.9: Comparison of experimental results at neutral and high pH

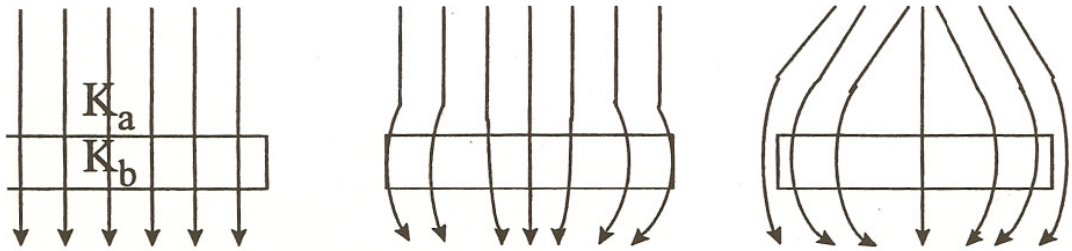

$K_b = K_a$ No streamlining	$K_a > K_b > (0.3\text{-}0.5)K_a$ Streamlining is weak	$K_b < 0.1\ K_a$ Streamlining is strong

Figure 5.1: Streamlining around a barrier – three scenarios

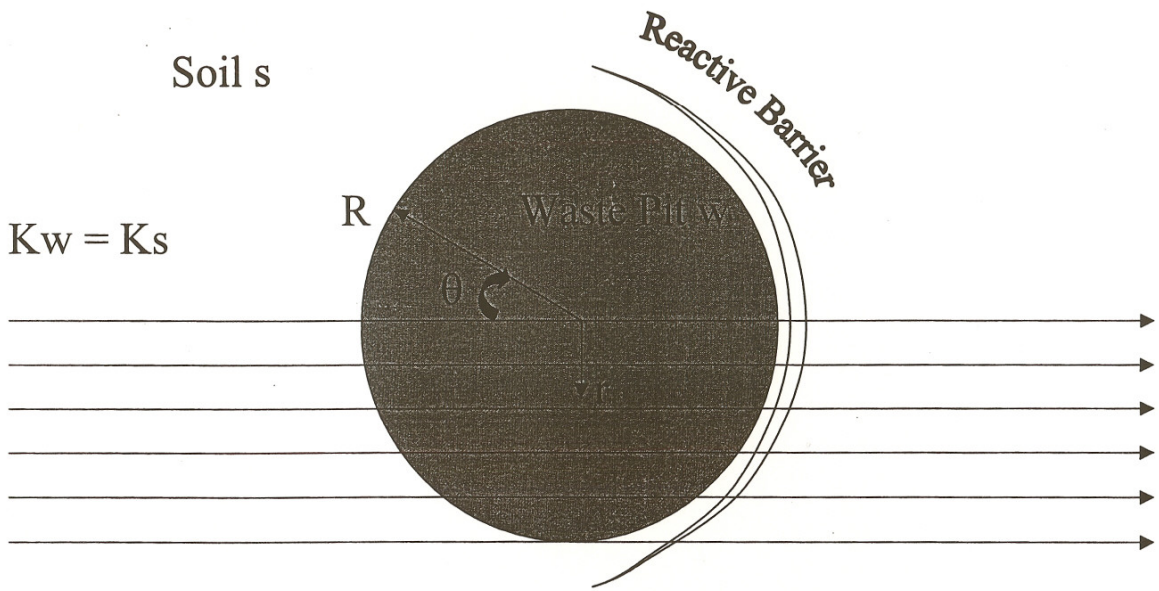

Figure 5.2(a): Flow around and within a waste depository – for $K_w = K_s$, the flow field is characterized by straight lines

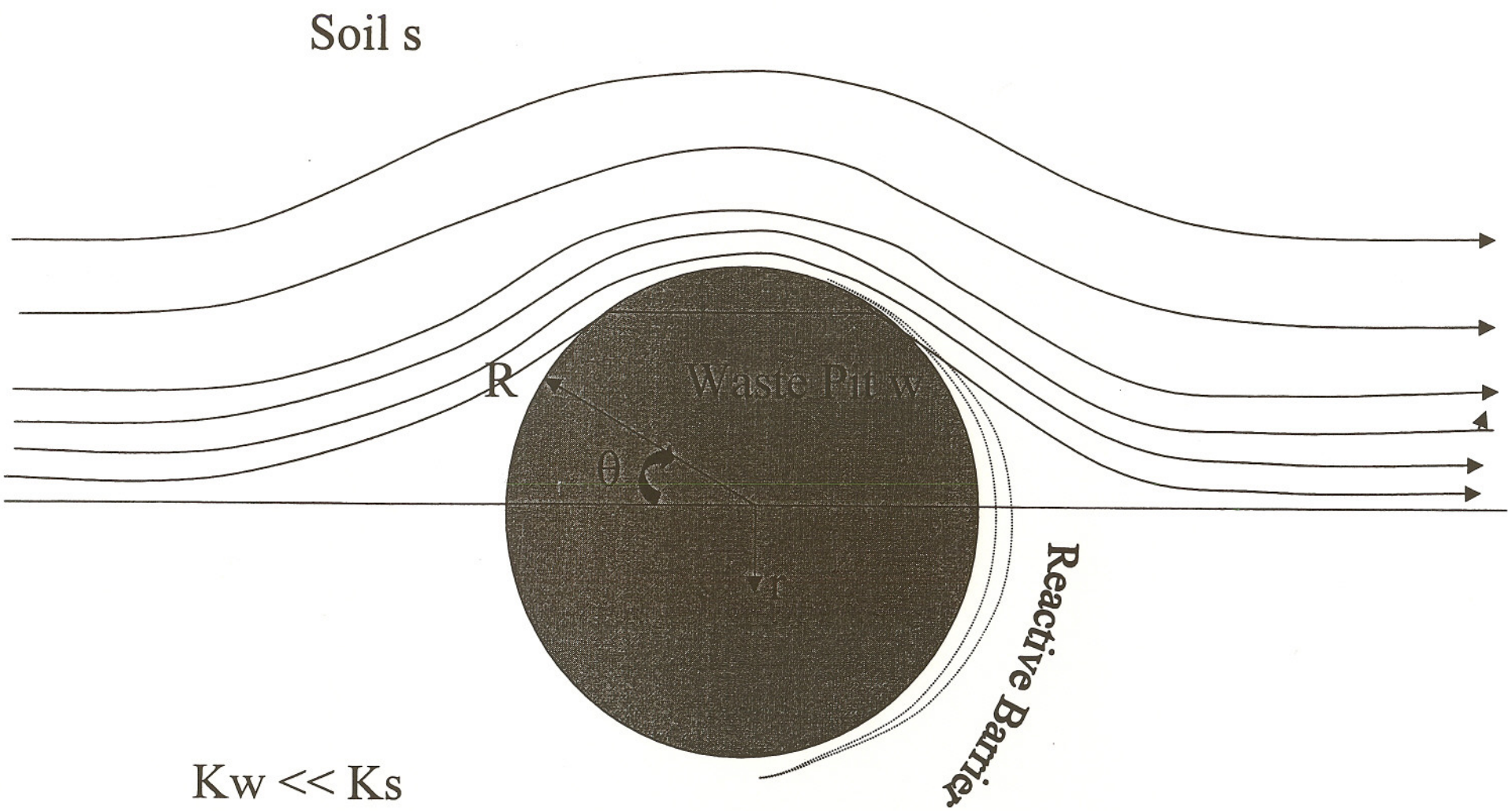

Figure 5.2(b): Flow around and within a waste depository – for $K_w < K_s$, the flow upstream of depository is divergent and downstream of it is convergent

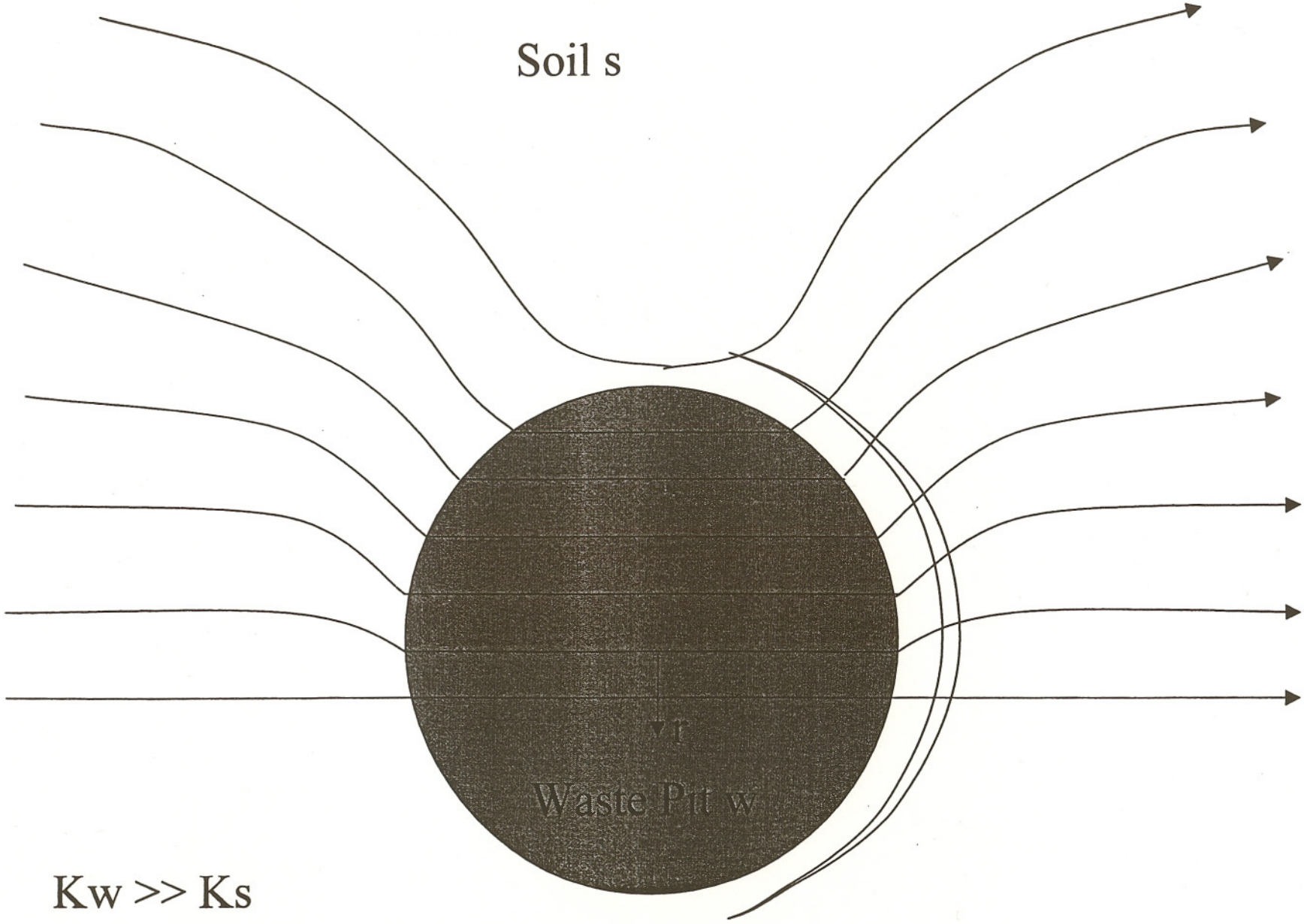

Figure 5.2(c): Flow around and within a waste depository – for $K_w > K_s$, the flow upstream of depository is convergent and downstream of it is divergent

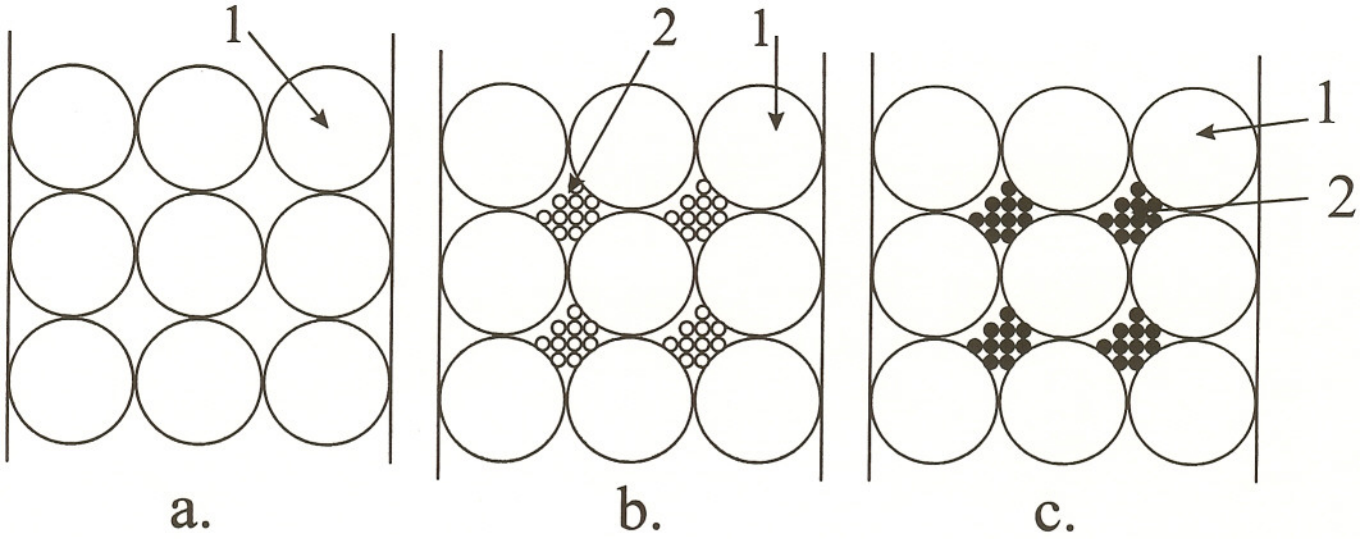

a. The porosity is maximum in the packed bed of mondisperse particles.

b. The porosity decreases in the polydisperse powder case because the smaller particles occupy space in pores between larger particles. There is a small space for RM in pores of a polydisperse soil (sand). [1. Soil large particles, 2. Soil small particles]

c. After removal of fine fractions from soil, the pores between larger soil particles increase and the space for RM and for water flow increases. The larger the dimension of coarse particles remaining after small fraction separation, the larger will be the RM volume fraction and therefore, larger HC. [1. Soil (sand) large particles, 2. RM particles occupy space remaining after small soil particle removal]

Figure 5.3: Importance of removing smaller soil particles for increasing RM volume fraction in RM/sand mixture

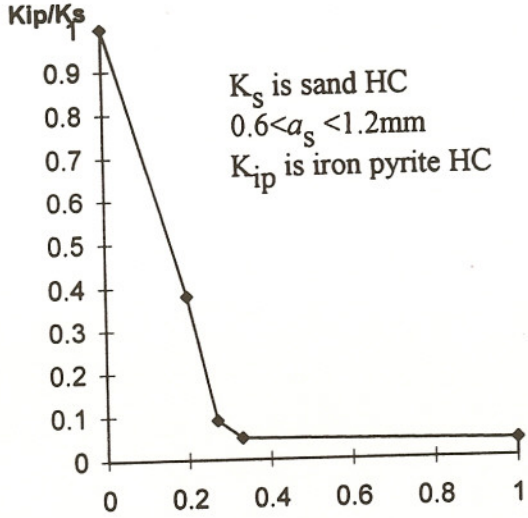

Figure 5.4(a): Dependence of HC of coarse sand RM mixture on RM volume fraction

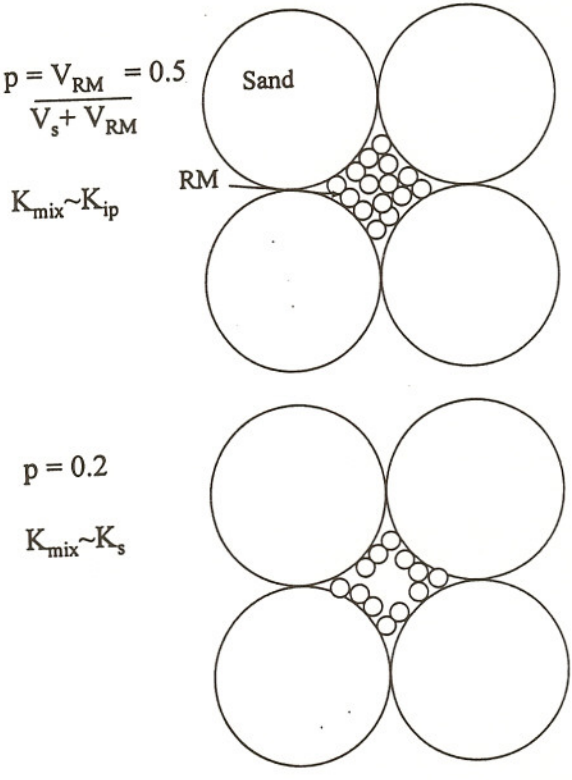

Figure 5.4(b): Illustration of the mechanism of the influence of pore filling with smaller particles on coarse sand hydraulic conductivity

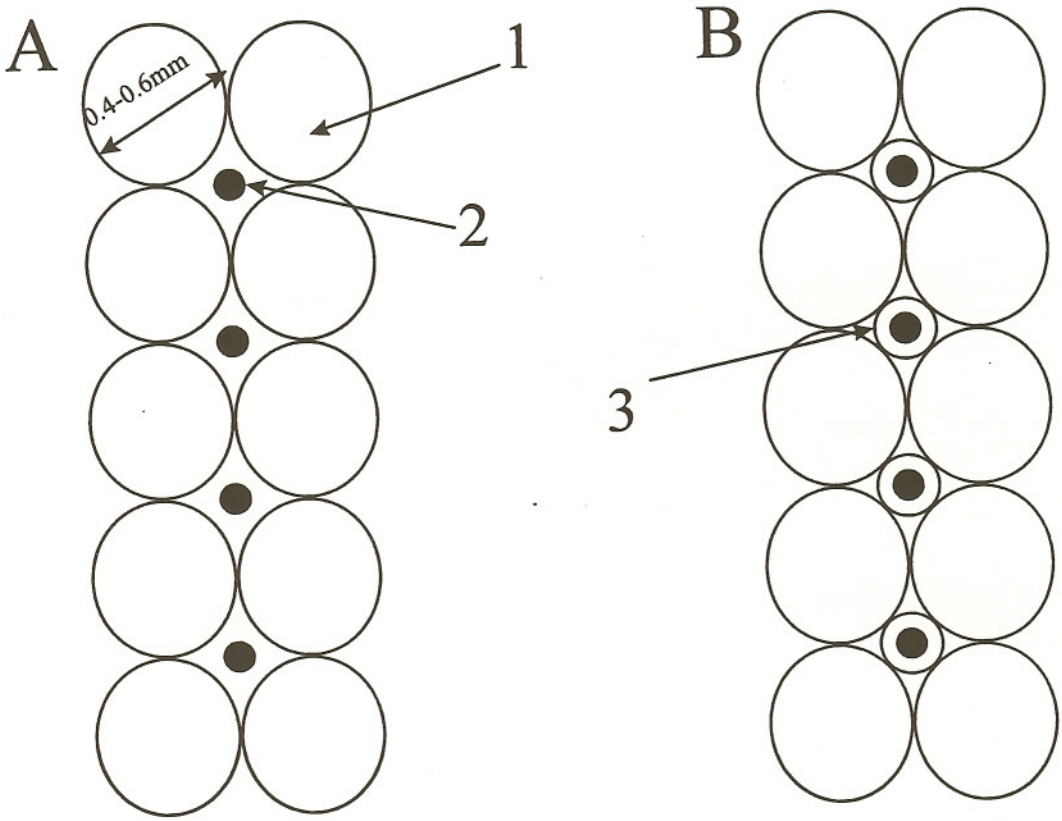

A. Sand with narrow size distribution and particles' dimensions 0.4-0.6 mm. Pores filled with RM particles with dimensions around 0.1 mm.

B. Pores are clogged mainly with either reduced chromium compound or with calcium deposit.

Almost every pore between sand particles is filled with a particle of RM that causes strong retardation of GW flow. A further decrease in hydraulic conductivity is caused by the decrease in free space in pores for GW flow, as reduced chromium compound or calcium deposit covers RM particle surface. This kind of mixing is not favorable for a barrier installation using RM/sand (soil) mixture. [1. Sand, 2. RM particle, 3. Deposit]

Figure 5.5(a): Weak vs. almost ideal mixing – schematic illustration of almost ideal mixed RM with almost monodisperse sand (soil) fraction

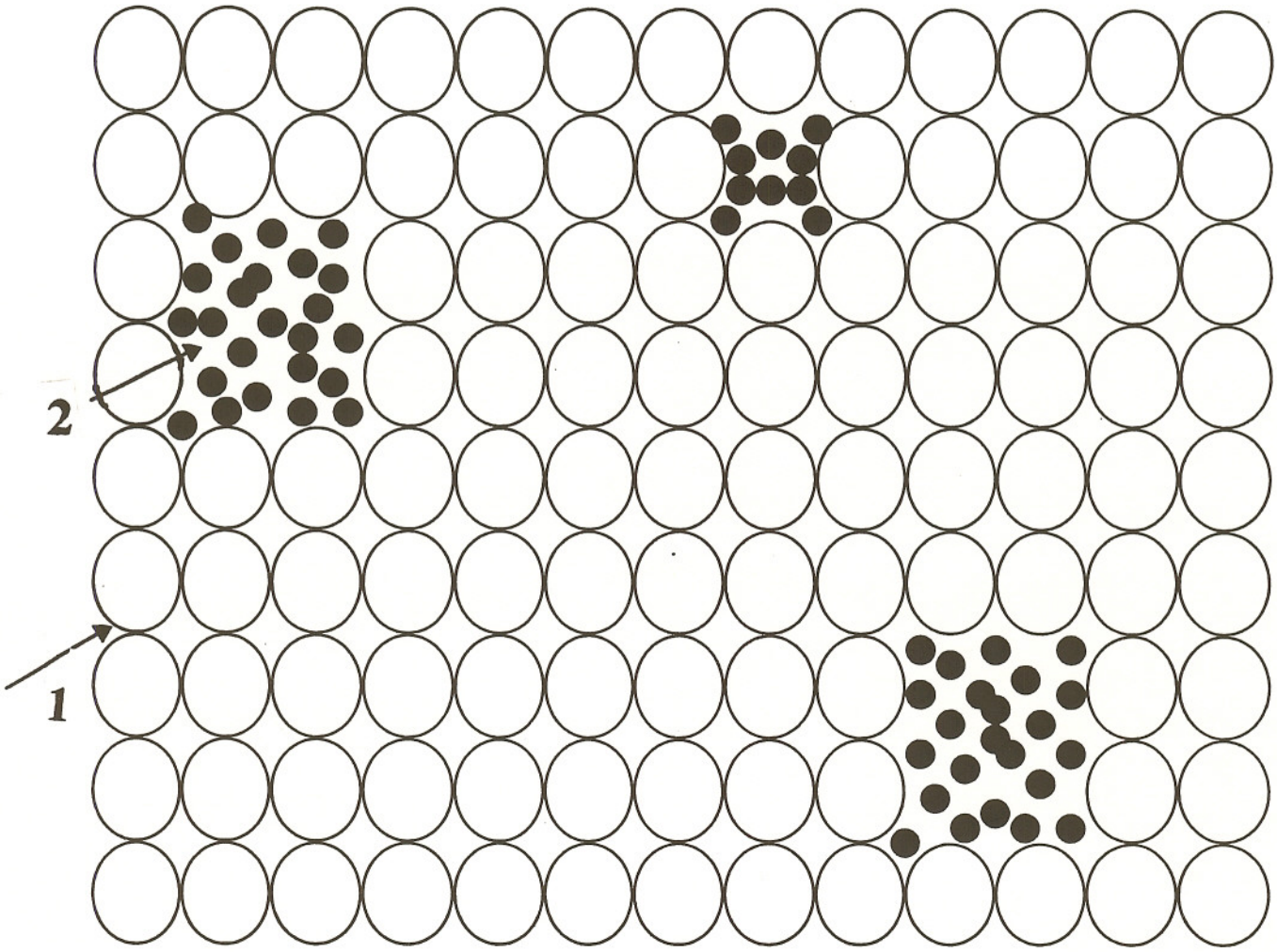

The complete separation of RM particles and their uniform distribution between sand particles is not achieved at weak mixing. RM particle portions (RMPP) with dimensions of 0.2-0.8 mm are preserved and randomly distributed within sand particles. Addition of RM in the form of RMPP to sand causes a minor decrease in hydraulic conductivity because the majority of transport channels (pore sequence) for water transport is preserved. [1. Sand particles, 2. RM particle portions consisting of 10-1000 RM particles]

Figure 5.5(b): Weak vs. almost ideal mixing – schematic illustration of weak mixed RM with almost monodisperse fraction of sand (soil)

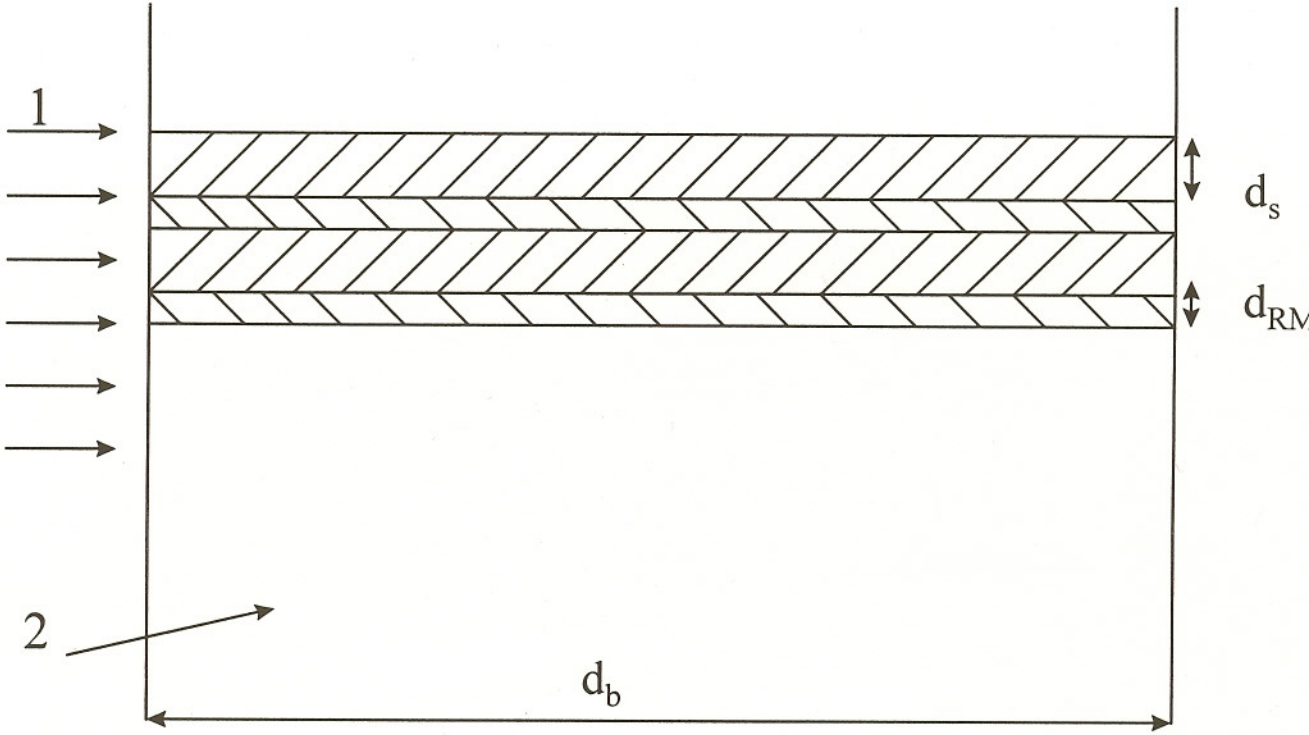

The layer of soil coarse fraction or coarse sand has a large HC decline that provides a large HC of barrier as a whole and prevents bypassing. This high barrier HC is preserved even at very strong HC decline within RM layer caused by chromium accumulation because GW moves mainly within sand layer and HC declination occurs within RM layer. During the residence time, chromium diffuses from sand layer into RM layer where its reduction and accumulation takes place. [1. GW stream, 2. PRB layered structure, d_s = soil layer thickness, d_{RM} = RM layer thickness, d_b = PRB thickness]

Figure 5.6: Schematic of RM/soil layered structure

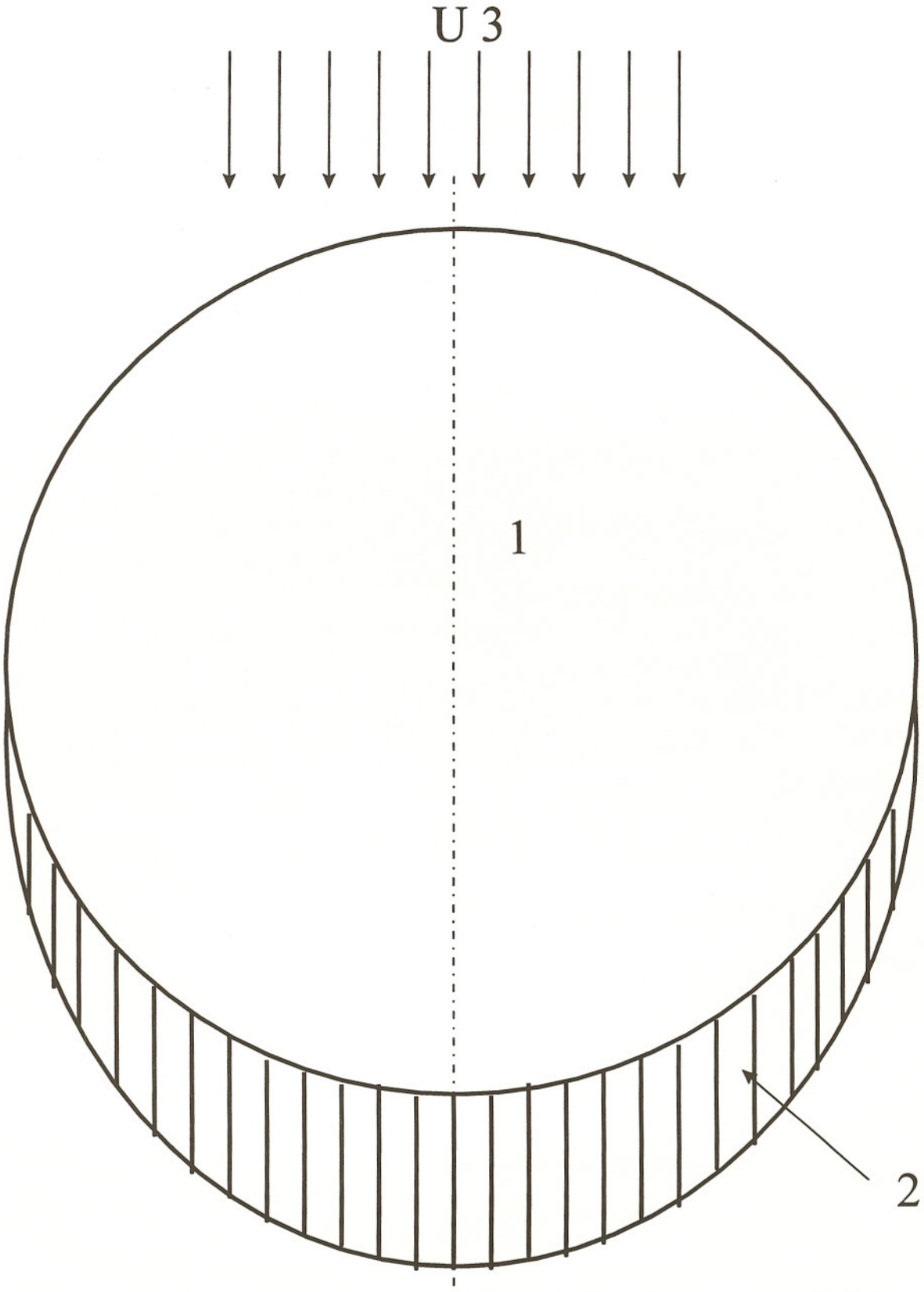

[1. Depository, 2. Barrier of variable thickness, 3. Groundwater stream velocity]

Figure 6.1: Schematic of variable thickness barrier in continuous configuration

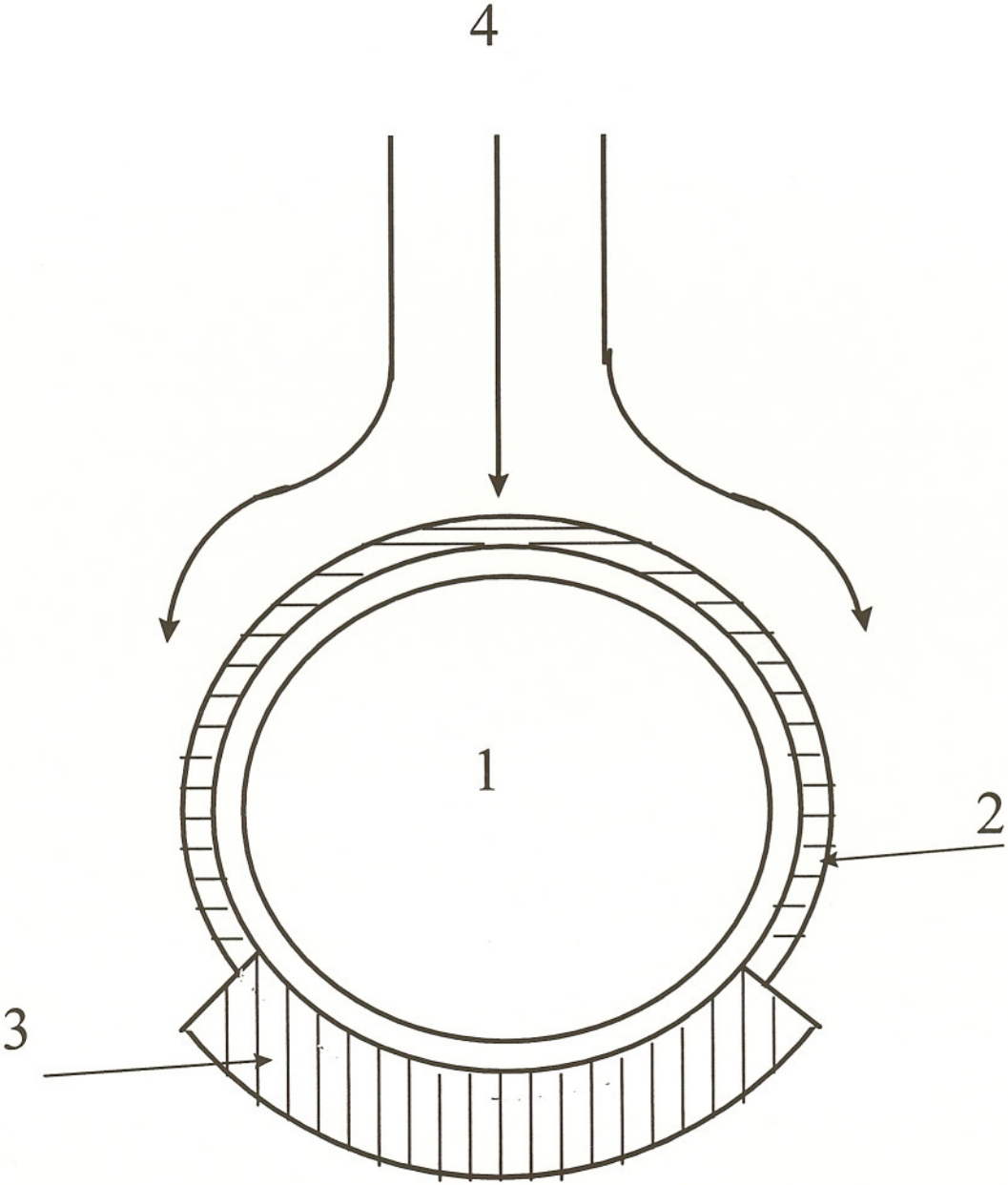

[1. Depository, 2. Upstream cutoff wall, 3. PRB, 4. GW stream]

Figure 6.2: Schematic of barrier configuration supplemented with upstream cutoff walls

Appendices

APPENDICES

A.1. Appendix 1

A.1.1. Importance of Individual Investigations of Passivation Kinetics and Hydraulic Conductivity Decline Regarding Individual Characteristics of Every Site

The reduction of passivation and corrosion is very difficult to quantify. One concludes that RMC dependence on flow rate and influent concentration needs to be investigated with experiment. With account for long term character of these experiments the parallel investigations with different pair values (velocity, concentration) are necessary. Even with 10 parallel experiments a rather small number of combinations of values for velocity and influent concentration is possible. The velocities and concentrations for the three sites vary in rather wide range. Since the function describing the RMC dependence on velocity and concentration will be not exact, the more reliable approach is the individual modeling with account for the individual characteristic of a given site. Even with this approach, a lot of parallel measurements are necessary. Even with a single value for groundwater concentration, the large seasonal variation in velocity creates the necessity of parallel experiments with at least 3 values for velocity, namely: minimum, maximum and medium. In addition, the experiments with concentrations smaller than that of site groundwater are desirable because any layer inside the barrier is initially filled with groundwater with decreased effluent concentration produced with upstream layers. Thus the procedure of the RM suitability for a definite site consists of 2 stages:

1. The preliminary evaluation based on the RMC dependence on concentration and velocity. The error of this preliminary evaluation can be very large with account for many difficulties discussed above.
2. The more exact final evaluation based on the individual modeling with account for a site individual characteristics.

A.1.2. Complications in Reactive Barrier Modeling Caused by Seasonal Variation in Groundwater Velocity

Is there a correlation between chromium concentration and seasonal variation of groundwater velocity? The seasonal variation in groundwater velocity is large and correspondingly the large variation can arise in the prediction of critical barrier capacity if the maximum or the minimum velocity will be substituted in equation [5.2]. Neither the minimum nor the maximum velocity has to be used in this prediction. According to the general definition of RBC, it is the total amount of chromium in groundwater stream crossing the barrier during 1 year divided by the barrier length and multiplied by the entire duration of barrier life, T_b .If the velocity changes and can be represented as a function of time, equation [5.2] has to be generalized:

$$\frac{n_i}{d_b}\int_0^{year} u_b(t)dt \sim \frac{n_i}{d_b}\sum u_{bk}\Delta t_k \qquad [A.1.1]$$

and

$$\sum_{k=1}^{m}\Delta t_k = 1year \qquad [A.1.1a]$$

Since, the velocity as a function of time is measured some times per year, it can be characterized with this different discrete value. This value has to be related to the time intervals between measurements, Δt_k. If the maximum and the minimum velocities are known then there are only 2 time intervals. But the maximum and minimum velocities cannot be found without

many measurements with small time intervals between them. With very little information about groundwater stream, the situation can be evaluated as there is an equal time for the maximum and the minimum velocity. This leads to a simple result with a large error.

$$C_b = \frac{n_b}{d_b} \frac{u_{\min} + u_{\max}}{2} T_b \qquad [A.1.2]$$

Naturally, more information about seasonal variation for groundwater velocity is necessary. It may happen that the seasonal variations in velocity cause seasonal variations in concentration. The rainwater mixing with chromium contaminated water leads to chromium dilution and chromium concentration decrease. The mixing is possible even as rainwater layer is formed due to infiltration above the contaminated layer. The mixing occurs as both layers slowly move in the horizontal direction due to the head gradient. The mixing occurs as small stream envelopes a soil particle or an agglomerate and splits into 2 streams. This mixing occurs on the boundary between 2 large streams, namely: groundwater stream and fresh rainwater stream. As a result, the boundary between these layers becomes wider with the decreased chromium concentration.

A.2. Appendix 2: Weak Bypassing Mechanism – Qualitative and Semi-quantitative Considerations (Numerical Calculations)

A continuous barrier cross-section and a profile for hydraulic head are shown in Fig. A.2.1. As there is no difference in barrier and aquifer conductivities, the hydraulic gradient (HG) inside the barrier is identical with the regional hydraulic gradient (line 1). As the barrier conductivity is smaller than that of aquifer:

$$K_b < K_a \qquad [A.2.1]$$

the HG inside the barrier has to be increased to provide the GW flux through the barrier approximately the same as at large distance before the barrier. This occurs in the most interesting case of weak bypassing; that means that the GW is mainly flowing through the barrier, i.e. the barrier installation causes a weak change in hydraulic field only.

The mechanism of the HG increase inside the barrier is clear. As GW meets larger hydrodynamic resistance entering the barrier, the head grows up before the barrier (curve 2). Correspondingly, head decreases behind the barrier. This head increase (decrease) is an unknown function of distance to the barrier surface, $h_1(z)$. Naturally, it decreases with the increasing distance to the barrier because at rather large distance, the regional gradient is realized. The dependence of z on h_1 is shown qualitatively in Fig. A.2.1.

The additional head changes along the barrier as well, i.e. it is a function of coordinate x and $h_1(z,x)$. As the barrier length is L, we nominate $x = 0$ in the barrier center and correspondingly $x = L/2$ at the barrier's edge. The additional head arises due to the presence of a barrier. It means it is negligible far from barrier in x direction as well. It does not mean that the additional head h_1 is absent near the barrier edge. But it is smaller there, i.e. h_1 is the function with its maximum at $x = 0$ and monotonous decrease with the increasing x. This HG decrease along the barrier causes GW flow from the barrier center to its edges, $x = \pm L/2$. This tangential (regarding the barrier) flow is the first step of bypassing. This flow behind the barrier edges bypasses it. This simplified picture enables to evaluate the bypassing dependence on the barrier thickness, d_b and length. The tangential HG can be evaluated as a ratio, $h_1(z,0)/(L/2)$, the normal gradient as $2h_1(0,x)/d_b \sim 2h_1(0,0)/d_b$. Now the entire normal flow can be evaluated as:

$$I = K_b \frac{2h_1(0,0)}{d_b} L \qquad [A.2.2]$$

and the entire tangential flow as:

$$I_s = \frac{2K_a h_1(0,0)}{L} \varepsilon \cdot L \qquad [A.2.3]$$

where ε is an unknown multiplier. The calculation of the entire tangential flow needs information about z dependence for $h_1(z,x)$. Since the latter is absent, we assume that h_1 is non- zero within distance L from the barrier and correspondingly the tangential flow extends over this distance. It means that the entire tangential flow is proportional to L. However, the larger the value of z, the smaller the value of h_1 and its tangential derivative, i.e. the tangential flux density is evaluated with the use of $h_1(0,0)$ instead of $h_1(z,0)$. It means that the coefficient ε introduced in Eq. [A.2.3] for the correction is smaller than 1. The bypassing can be evaluated as a ratio of the total tangential flow to the total flow through the barrier, i.e.

$$\frac{I_s}{I} \sim \varepsilon \frac{d_b}{L} \cdot \frac{K_a}{K_b} \qquad [A.2.4]$$

Note that this evaluation does not comprise the case of extremely weak bypassing, namely the case of small difference between barrier and aquifer conductivities. In this case the normal flux is proportional to the regional gradient because h_1 is extremely small. We neglected this term assuming that h_1 is not very small that caused the cancellation of unknown $h_1(0,0)$ at the ratio [A.2.4] evaluation. To provide this cancellation, the case $(K_a - K_b) << K_a$ was excluded. The numerical calculations confirmed this quantitative picture (Fig. A.2.2). Bypassing is characterized with GW trajectories obtained with numerical calculation. The contaminant loss increases with increasing barrier thickness as illustrated in Fig. A.2.3. The contaminant loss decrease with increasing barrier length as illustrated in Fig. A.2.4.

A.3. Appendix 3: Streamlining Around Circular Waste Depository

A set of simplification is used to make the analytical solution easier. A flat horizontal surface of aquitard and isotopic aquifer HC uniform in space are assumed. At this condition the hydrodynamic velocity does not depend on the elevation head Z and the GW flow field can be described by two dimensions. The steady state conditions for GW are assumed. Correspondingly, the steady state Laplace equation for hydraulic head can be used:

$$\frac{\partial^2 h}{\partial r^2} + \frac{1}{r} \cdot \frac{\partial h}{\partial r} + \frac{1}{r^2} \cdot \frac{\partial^2 h}{\partial \theta^2} = 0 \qquad [A.3.1]$$

where the cylindrical system of coordinate is characterized in Fig. 5.

Eq. [A.3.1] has to be considered inside and outside of the depository where the hydraulic conductivities are different. Thus, the hydraulic head distribution inside a depository, $h_w(r,\theta)$ and outside of it $h_s(r,\theta)$ have to be introduced. Both distributions satisfy Laplace equation [A.3.1]. Its solution can be obtained with the method of independent variable separation, namely in the form:

$$h(r,\theta) = R(r)\Theta(\theta) \qquad [A.3.2]$$

This expression substitution into equation [A.3.1] yields ordinary differential equations for functions R and Θ.

$$r \frac{d}{dr}(r \frac{dR}{dr}) - n^2 R = 0 \qquad [A.3.3]$$

$$\frac{d^2\Theta}{d\theta^2} + n^2\Theta = 0 \qquad [A.3.4]$$

Their solutions are $R_n(r)$ and $\cos n\Theta$, $\sin n\Theta$, where $n = 1,2....$ At large distance from depository upstream, the hydraulic gradient distribution is determined by the regional hydraulic gradient value, V_s, i.e.

$$h(r,\theta) = V_s r \cos\theta \qquad [A.3.5]$$

This enables us to satisfy the conditions on the boundary between soil and depository i.e. $r = R$

$$h_s(R,\theta) = h_w(R,\theta) \qquad [A.3.6]$$

$$K_s \frac{dh}{dr}(R.\theta) = K_w \frac{dh_w}{dr}(R,\theta) \qquad [A.3.7]$$

using the solutions of the form:

$$h_s(r,\theta) = R_{1s}(r)\cos\theta, h_w(r,\theta) = R_{1w}(r)\cos\theta \qquad [A.3.8],[A.3.9]$$

and to specify equation [A.3.3] with $n = 1$. The hydraulic head and GW flow density have to be continuous at the crossing of the boundary between soil and aquifer, i.e. at $r = R$. These conditions are expressed with equations [A.3.6] and [A.3.7]. Since,

$$R_{1s} = \frac{1}{r}, R_{1w} = r \qquad [A.3.10]$$

the solutions have to be sought as:

$$h_s = V_s[r + \frac{R^2}{r}(1+x)]\cos\theta \qquad [A.3.11]$$

$$h_w = V_w \cos\theta \qquad [A.3.12]$$

The substitution of these functions into the boundary conditions [A.3.6] and [A.3.7] transform them into linear algebraic equation for 2 unknowns, V_w and x. The solution of this system is:

$$x = -\frac{2K_w}{K_s + K_w} \qquad [A.3.13]$$

$$V_w = \frac{2K_s}{K_w + K_s} V_s \qquad [A.3.14]$$

With $K_w = K_s$, the solutions [A.3.11] and [A.3.12] have to be reduced to unidirectional distribution [A.3.5]. This qualitative consideration is confirmed by the substitution, $x = -1$, that follows from equation [A.3.13] into equation [A.3.11]. At this substitution, equation [A.3.11] reduces to equation [A.3.5]. At equal hydraulic conductivities $V_w = V_s$, according to equation [A.3.14], that transforms the distribution [A.3.12] into [A.3.5] as well. The GW flux into (out) a depository has to be absent if its HC is equal to zero ($K_w = 0$). This leads to $x = 0$, according to equation [A.3.13] and this in turn leads to zero value for $dh_s/dr(R)$, according to equation [A.3.11], i.e. to zero flux within the depository. The total stream of GW into depository is obtained by means of integration over its boundary in the range, $0 < \pi/2$:

$$Q = \int_0^{\pi/2} 2\pi R^2 K_s \frac{\partial \cdot h_s}{d \cdot r} \sin\theta d\theta = 2\pi R^2 K_s V_s x \int_0^{\pi/2} \cos\theta \sin\theta d\theta = \pi R^2 u_s \frac{2K_w}{K_w + K_s} \qquad [A.3.15]$$

A.3.1. Bypassing of Arc Like Barrier

If a barrier is installed as an arc along the depository boundary downstream, a new boundary condition along this boundary arises:

$$K_s \frac{\partial \cdot h_s}{\partial \cdot r}(R) = K_b \frac{h_s(R) - h_s(R+d_b)}{d_b} \qquad [A.3.16]$$

We assume that the barrier is sufficiently thin, i.e.

$$d_b << R \qquad [A.3.17]$$

that yields the representation for hydraulic gradient inside a barrier as r.h.s. of equation [A.3.16]. The equation [A.3.16] means that the flux from the depository into the barrier (l.h.s.) equals to the flux across the barrier (r.h.s.). The special case is of interest, corresponding to weak bypassing. This restriction enables the application of the method of sequent approximation. The solution is sought as the superposition of zero approximation and the first approximation, h_1:

$$h = h_0 + h_1 (r, \theta) \qquad [A.3.18]$$

$$h_1 << h_0 \qquad [A.3.19]$$

where h_0 describes the distribution before a barrier installation, i.e. h_0 is characterized by equation [A.3.11]

$$h_{os} = V_s[r + \frac{R^2}{r}(1+x)]\cos\theta \qquad [A.3.20]$$

and

$$h_{s1} = V_{s1}\frac{R^2}{r}\cos\theta \qquad [A.3.21]$$

This substitution into equation [A.3.16] yields:

$$V_s K_s x = \frac{K_b}{d_b}(V_s x d_b + 2V_{s1}R) \qquad [A.3.22]$$

The first term in bracket is:

$$h_{os}(R+d_b) - h_o(R)$$

and the second term is:

$$h_{s1}(R+d_b) - h_{w1}(R)$$

It is clarified from Fig. A.2.1 that a barrier installation causes a hydraulic head increase before barrier and its decrease after the barrier and their absolute values are equal. Equation [A.3.21] relates to $r > (R + d_b)$. It means, that:

$$h_{w1}(R,\theta) = -V_{s1}R\cos\theta \qquad [A.3.23]$$

and correspondingly,

$$h_{s1}(R+d_b,\theta) - h_{w1}(R,\theta) = 2V_{s1}R\cos\theta \qquad [A.3.24]$$

Substituting into equation [A.3.22], we obtain:

$$\frac{V_{s1}}{V_s} = \frac{d_b}{R}\cdot\frac{K_w}{K_s + K_w}(1 - \frac{K_s}{K_b}) \qquad [A.3.25]$$

As barrier and soil conductivities are equal, a barrier installation does not change hydrodynamic field, i.e. the term, h_{s1} has to be absent, that is confirmed with equation [A.3.25]. At $K_b < K_s$ and $K_b > K_s$, the GW stream through the barrier is larger and smaller than before its

installation; that is confirmed with equation [A.3.25]. As the waste conductivity is zero, there is no GW flow inside it and consequently through the barrier. As there is no flux through the barrier the distribution, h_{s1} does not arise, that is confirmed with equation [A.3.25].

The distributions [A.3.20] and [A.3.21] are identical at $r = R$ with a difference in V_s and V values. Their substitution into equation [A.3.15] yields the entire flux of GW through the aquatory. At barrier conductivity larger than that of soil this flux decreases and this decrease is equal to the entire bypassing flow. Thus equation [A.3.25] yields the ratio of the entire bypassing flow and the entire flow. This ratio is called contaminant loss ratio because the contaminant in bypassing flow does not cross barrier and is lost for the barrier remediation. Equation [A.3.25] is a first crude approximation and has to be perfected with account for the boundary condition along the depository boundary upstream. The solution has to be a superposition of term, proportional to $cos\theta$ and $sin\theta$, because the anti-symmetry of distribution, characterized by using $cos\theta$ only is violated due to difference in conditions for depository boundaries downstream and upstream. On the l.h.s. of equation [A.3.16] a term was omitted namely the flux outside the depository caused with appearance the additional head drop h_{s1}. This term is $V_{s1}\ R/R$ and it is smaller than term $V_{s1}\ R/d_b$ on the r.h.s. of equation [A.3.22].

A.4. Appendix 4: Evaluation of Small Decrease in HC and in Transport Step Rate of Chromium Reduction at Optimal Weak Mixing of RM and Sand

To evaluate this small decrease, let us introduce a mean radius for RM particle portion (RMPP), i.e. let us neglect their distribution regarding the dimension and the deviation of their shapes from spherical one. As the HC inside RMPP decreases very much we can neglect it, i.e. HC for RMPP equals to zero. Thus, the formulation of task is that there was an initial HC of RM/sand mixture $K_{mix}(p_{opt})$ and afterwards RMPP becomes impermeable due to either chromium reduction or due to Ca deposit formation. Thus, there is a disperse system with impermeable spherical inclusions and their volume fraction is p_{opt} and the equation for its HC as a function of p_{opt} is necessary.

The analogy between hydrodynamics of porous media and dielectric properties of disperse system [43] can be used that enables us to apply the well known Maxwell equation:

$$\delta\varepsilon = \bar{\varepsilon} - \varepsilon_o = \frac{3\varepsilon_o(\varepsilon_1 - \varepsilon_o)}{2\varepsilon_o + \varepsilon} p \qquad \text{[A.4.1]}$$

where ε_o and ε_1 are the dielectric permitivities of media and particles, respectively, $\bar{\varepsilon}$ is the mean dielectric permitivity of mixture and $\delta\varepsilon$ is the decrease of dielectric permitivity caused with particle presence. In our case HC is an analog of the dielectric permitivity. Correspondingly, an analog of equation [A.4.1] is:

$$\delta K = K_{mix}(p_{opt}) - K_s = \frac{3K_s(K_{RMPP} - K_s)}{2K_s + K_{RMPP}} p_{opt} \qquad \text{[A.4.2]}$$

where $K_{mix}(p_{opt})$ is HC of RMPP/sand mixture after HC of RMPP is decreased due to the formation of either chromium deposit or calcium oxide deposit. As small HC of RMPP can be neglected, we obtain:

$$\delta K / K_s = -\frac{3}{2} p_{opt} \qquad \text{[A.4.3]}$$

The HC decrease is not large even at $p_{opt} = 0.2$, namely 0.3.

The so called "principle of generalized conductivity" is used and extended above over HC of porous media. It is described in Chapter 6, paragraph 2 of reference (43). The principle comprises of electrostatics, electrodynamics, magnetostatics, thermal conductivity and diffusion. This series is supplemented now with HC. Each of the different fluxes, j satisfies the continuity equation:

$$div\,\vec{j} = 0 \qquad [A.4.4]$$

and is a linear function of the corresponding vector field, $\vec{x}$:

$$\vec{j} = \Lambda\,\vec{x} \qquad [A.4.5]$$

where Λ are phenomenological or kinetic coefficients. In our case j is GW velocity, x is hydraulic head, Λ is HC, and equation [A.4.6] is Darcy law.

$$Q = K\,\mathrm{grad}p \qquad [A.4.6]$$

For any nature of conductivity process, the boundary conditions are the equality of the normal components of fluxes on both sides of the interfaces, i.e.

$$j_{1n} = j_{on}, i.e. \Lambda_1 x_{1n} = \Lambda_o x_{on} \qquad [A.4.7]$$

and equality of thermodynamic forces:

$$x_1 = x_o \qquad [A.4.8]$$

These boundary conditions are similar to our boundary conditions [A.3.6] and [A.3.7]. The mathematical formulation of the principle of generalized conductivity is:

$$\frac{\overline{\Lambda}}{\Lambda_o} = F(p, \frac{\Lambda_o}{\Lambda_1}) \qquad [A.4.9]$$

where Λ_0 and Λ_1 are media and particle conductivities and Λ is the disperse system conductivity. For small volume fraction and for dielectric permitivity, the general equation [A.4.9] is specified as Maxwell equation [A.4.1]. This enables us to apply an analog of Maxwell equation to HC, i.e. to write equation [A.4.2].

The chromium reduction is a two-step process. The first step is chromium transport from local stream of GW on a RM particle surface. The second step is chromium ion reduction on this surface. At RM/sand mixture preparation with a weak mixing, the transport step becomes slower than in ideal mixture. However, it can be sufficiently rapid at proper weak mixing. The transport step becomes slower because when the mean path for chromium transport to RM particle surface is larger, the mixing is weaker.

For evaluating the role of transport rate, the comparison of 2 characteristic times is necessary, namely the GW residence time, t_{res} within a barrier and the mean time necessary for chromium ion transport to the RMPP surface, t_{dif}. This transport occurs due to molecular (ion) diffusion that is marked with index "dif".

Introducing a notion of mean diffusion path, b_D, the diffusion transport time can be evaluated using the well known equation of A. Einstein:

$$t_{dif} = \frac{b_D^2}{D} \qquad [A.4.10]$$

where D is chromium ion diffusivity. For a crude evaluation of b, let us consider a simplified model for the result of weak mixing. A mean linear dimension a for RMPP dimension is introduced, i.e. the real distribution of RMPP dimension is neglected.

A mean distance between single RMPP is introduced, i.e. the distribution regarding this

distance is neglected. Afterwards the well known cell model is applied, namely a spherical cell with a radius b is considered with RMPP in its center. The mixture as a whole is considered as a structure consisting of these elementary cells. It means that RM volume fraction in cells equals to RM volume fraction for a mixture as a whole, i.e.

$$\frac{a^3}{b^3} = p_{opt} \qquad [A.4.11]$$

or

$$b = ap_{opt}^{-3}$$

and

$$(b-a) = a(p_{opt}^{-3} - 1) \sim a \qquad [A.4.12]$$

The application of a cell model to replace the consideration of real transport processes with its description for one cell. The maximal diffusion path within a cell equals to b-a, i.e. the mean diffusion path is smaller. Nevertheless, the maximal diffusion path will be used that leads to an over evaluation of the mean diffusion time. Now with the substitution of a instead of b_D into equation [A.4.10], we obtain:

$$t_{dif} \sim \frac{a^2}{D} \qquad [A.4.13]$$

With ion diffusivity of 10^{-5} cm/sec, t_{dif} equals to 10^3 sec for $a \sim 1$ mm. Meanwhile, the residence time for a barrier is 10^5 - 10^6 sec. Thus, the residence time exceeds the time necessary for diffusion by 100 - 1000 times. The GW stream may enhance the diffusion transport. However, this increase is not essential because Pecklet number almost equals to 1.

$$Pe = \frac{au}{D} \sim \frac{0.1 \cdot 10^{-4}}{10^{-5}} \sim 1 \qquad [A.4.14]$$

This evaluation is crude, because the diffusion time has to be compared with GW residence time in one cell, which is 1000 times smaller than the residence time for a barrier. However, the chromium is consumed at GW transport through a series consisting of 1000 cells. This thousand compensates the preceding thousand. Naturally, this is a crude evaluation, as the chromium accumulation during GW stream through 1000 cells is replaced with one cell consideration only. However, the result is reliable because the residence time for a barrier exceeds the diffusion time 1000 times. More exact quantification is possible using the theory of diffusion in bi-porous media.

As a real picture contains the elements of Figs. (5.5a) and (5.5b), the notion of mean quantity of particles for RMPP, N has to be introduced. It means that RMPP number is N times smaller than the total number of primary particles. If at ideal mixing almost all pores between sand particles are filled with RM particles, the preservation of their RMPP during weak mixing means that the percentage of pores filled with RMPP will be N times smaller at ideal mixing. The value N = 3 - 5 is sufficient to prevent large decrease in hydraulic conductivity. N = 3 - 5 means, that 1 pore among 3 - 5 pores is filled with RMPP, i.e. there is 2 - 4 free pores in the vicinity of almost any free pores and only one adjacent pore is clogged. As other adjacent pores are free, the local water stream will change its direction, i.e. the bypassing is possible. This repetition of bypassing many times along a water streamline will produce some decrease in HC. The smaller the HC, the larger is the number, N (smaller RMPP concentration).

A.5. Appendix 5: Conditions of RM/Sand Mixture and their Suitability for Barrier Installation with Minimal Bypassing

This problem arises if dry mixing will be used instead of recommended wet mixing.

A.5.1. Bypassing Around Barrier and Its Critical Thickness

A barrier with an invariant thickness, d_b and hydraulic conductivity, K_b is considered. The barrier has an arc shape with an angle of $\pi/2$. The hydrodynamic task pertaining to this problem is formulated and solved in Appendix 3 for the first crude approximation. The results are discussed here.

The GW stream entering the WD splits into 2 parts, one flowing through the barrier and the other bypassing it. The first stream is cleaned and the second stream preserves the initial chromium concentration, namely that in aquifer. If the barrier HC is smaller than the soil HC, bypassing is not avoidable. The question arises: how much bypassing is admissible?

The bypassing is not harmful if the entire amount of chromium in bypassing flux, i.e. $I_s n_i$ does not exceed that in GW cleaned with the barrier:

$$\frac{I_s n_i}{I n_{eff}} \leq 1 \qquad [A.5.1]$$

where I and I_s are fluxes into WD and around the barrier, respectively.

Fresh iron pyrite mixture can provide effluent concentration around 0.1 ppm. In the barrier, the back layer remains fresh even as the barrier volume is contaminated 99% (Section 6). Thus for n_{eff}, its value of 0.1 can be substituted into equation [A.5.1] to yield:

$$3 \cdot 10^{-3} < \frac{n_{eff}}{n_i} < 10^{-2} \qquad [A.5.2]$$

for 15 ppm < n_i < 50 ppm that corresponds to dissolved chromium concentration for different sites. Combining equations [A.5.1] and [A.5.2], we obtain:

$$\frac{I_s}{I} < 3 \cdot 10^{-3} - 10^{-2} \qquad [A.5.3]$$

In Appendix 3, bypassing dependence on the parameters characterizing a barrier and a depository is obtained which is combined with condition [A.5.3] as:

$$\frac{I_s}{I} = \frac{K_w d_b}{(K_w + K_s)R}(1 - \frac{K_s}{K_b}) < 3 \cdot 10^{-3} - 10^{-2} \qquad [A.5.4]$$

The equation is clear qualitatively. The thicker the barrier (larger d_b), the smaller is its hydraulic conductivity, K_b and stronger is the bypassing. At condition [5.8], i.e. at smaller soil conductivity, equation [A.5.4] becomes:

$$\frac{I_s}{I} \cong -\frac{K_s}{K_b} \cdot \frac{d_b}{R} \qquad [A.5.5]$$

Naturally, the conductivity ratio is important and not their absolute values. Two hydrodynamic resistances, namely that of waste depository (WD) and that of barrier are present in equation [A.5.5]. Hydrodynamic resistance is directly proportional to length and inversely proportional to HC, i.e. it is d_b/K_b for a barrier and R/K_w for a depository. The sequence of a depository resistance and a barrier resistance controls the GW stream through the barrier. If a barrier resistance is negligible in comparison with that of depository, the barrier does not influence on the GW flow, i.e. the bypassing caused with barrier is negligible. The larger the barrier resistance, the larger is its influence on GW flow within depository and the larger will be

the bypassing. This is expressed on the right side of equation [A.5.5], which is the ratio of barrier hydrodynamic resistance to that of WD.

Let us introduce the concept of critical barrier thickness, d_{bH} caused by the bypassing phenomenon.

$$d_{bH} = (3 \cdot 10^{-3} - 10^{-2}) R \frac{(K_w + K_s)}{K_w} (\frac{K_s}{K_b} - 1)^{-1} \qquad [A.5.6]$$

At a barrier thickness larger than d_{bH}, bypassing takes place. As the RM/sand mixture is used at a barrier installation,

$$K_b = K_{mix} = K_s / y \qquad [A.5.7]$$

where;

$$y = \frac{K_s}{K_{mix}(p_{opt})} > 1$$

This case only corresponds to bypassing. The specification of equation [A.5.6] with the use of equation [A.5.7] yields:

$$d_{bH} = (3 \cdot 10^{-3} - 10^{-2}) R (\frac{K_s + K_w}{K_w})(y - 1)^{-1} \qquad [A.5.8]$$

Table A.5.1. Critical barrier thickness for different K_s/K_w, R and y

$K_s/K_w \rightarrow$ R (m)$\downarrow$	0.3	1.0	3.0
		y = 2	
50	0.2 – 0.65	0.3 – 1.0	0.6 – 2.0
100	0.4 – 1.3	0.6 – 2.0	1.2 – 4.0
200	0.8 – 2.6	1.2 – 4.0	2.4 – 8.0
		y = 4	
50	0.07 – 0.22	0.1 – 0.33	0.2 – 0.7
100	0.13 – 0.4	0.2 – 0.7	0.4 – 1.3
200	0.23 – 0.7	0.4 – 1.3	0.8 – 2.6

A.5.2. Conditions for Remediation Using RM/Sand Mixture for Barrier Installation

Two critical thicknesses, d_{bH} and d_{bc} were introduced. A barrier thickness has to be larger than d_{bc} to provide the entire barrier capacity, i.e.

$$d > d_{bc} \qquad [A.5.9]$$

Also, the barrier thickness has to be smaller than d_{bH} to eliminate strong bypassing, i.e.

$$d < d_{bH} \qquad [A.5.10]$$

The information about the sites, namely its effective radius R, HC of surrounding soil, K_s, HC of waste, K_w, chromium concentration in GW stream, n_i and its velocity, u are necessary for the calculation of d_{bc} and d_{bH}. In addition, the long term investigations for the determination of RM capacity and HC for optimal RM volume fraction in mixture $K(p_{opt})$ are necessary. The comparison of the determined values for a barrier critical thickness can lead to 2 variants:

$$d_{bH} < d_{bc} \qquad [A.5.11]$$

and

$$d_{bH} > d_{bc} \qquad [A.5.12]$$

If case [A.5.11] takes place for a site, the RM/sand mixture is not suitable for a barrier installation. Indeed d has to exceed d_{bc} according to condition [A.5.9]. It means that d will exceed d_{bH}, according to equation. This corresponds to strong bypassing. Equation [A.5.12] is the condition for the possibility of remediation using RM/sand mixture for a barrier installation. Equation [A.5.12] allows us to choose the barrier thickness according to the rule:

$$d_{bH} > d > d_{bc} \qquad [A.5.13]$$

If d exceeds d_{bc}, the entire critical barrier capacity will be provided. If d is less than d_{bH}, the bypassing will be either absent or sufficiently weak.

A.6. Appendix 6: Nearly Uniform or Nonuniform Chromium Accumulation Within Barrier and Its Critical Thickness: Dynamics of Chromium Distribution within Barrier

The notion of critical barrier capacity which enabled us to introduce barrier critical thickness and therefore, to model long term performance of a barrier (Section 4) uses the assumption of uniform chromium distribution within a barrier. This assumption enables us to introduce the specific barrier capacity as:

$$c_{bcr} = C_{bcr} / d_b \qquad [A.6.1]$$

where C_{bcr} is the entire critical capacity of barrier. For nonuniform chromium distribution across a barrier the density of accumulated chromium is an unknown function of the distance to the barrier front surface. The notion of c_{bcr} according to equation [5.2] and the main condition [5.3] become useless. Correspondingly, the prediction of critical barrier thickness according to equation [5.19] becomes useless too.

There are no publications devoted to dynamics of chromium accumulation within the barrier. Even the assumption about uniform distribution which enables us to calculate barrier critical thickness is not introduced in the literature. The PRB dynamic model has to be elaborated using the conservation equation for chromium and the equation for reduction kinetics. These two equations enable us to calculate two non-steady distributions, one for accumulated chromium, $\rho(x,t)$ and the other for dissolved chromium, $n(x,t)$, where x is the distance to the barrier front surface (Figs. A.6.1 & A.6.2). The dynamic model in combination with accomplished measurement of chromium reduction kinetics (Section 4) confirms the assumption about uniform chromium distribution as a first approximation. The dynamics introduces an essential correction to this assumption. It is not valid for the whole barrier. It is valid for first layer only (Figs. A.6.1 & A.6.2).

The results of joint solution for two equations aforesaid can be formulated as a 3 layer dynamic model for the accumulated chromium distribution. The layer numeration corresponds to the direction of GW flow through a barrier. The chromium accumulated during the barrier life is located near the barrier front surface. This first layer can be called accumulation layer. The third layer adjacent to a barrier back surface almost does not contain any chromium. The second layer (located between first and third ones) can be called reduction layer because the reduction takes place within it. Indeed, there is no reduction within the first layer because it starts after the accumulation of maximum possible amount, C_{RM} in any cm^3. Also, there is no reduction in the third layer because it is reduced in the second layer.

The uniform distribution of chromium within layer 1 happens because the reduction stops at same accumulated chromium density $\rho(x) = c_{RM}$ for any $x < x_a(t)$, where $x_a(t)$ is the current thickness of accumulated layer. As there is no reduction within the accumulated layer, the dissolved chromium concentration does not change as GW flows through this layer, i.e. its concentration equals to initial one within the layer.

$$n(x,t) = n_i \qquad x < x_a(t) \qquad [A.6.2]$$

$n(x,t)$ decreases rapidly as GW flows through the second layer because of its reduction and accumulation. $n(x,t)$ approaches to the effluent concentration within third zone.

$$n_e < n(x,t) < n_i \qquad \{x<x_r(t)\} \qquad [A.6.3]$$

$$n(x,t) \sim n_e \qquad \{x_r(t)<x<d_b\} \qquad [A.6.4]$$

where $x_r(t)$ is the boundary between second and third layers. The shape and thickness of the second layer do not change with time. Its thickness is small in comparison with d_b and the entire amount of chromium accumulated within a barrier can be identified with the accumulation in the first layer.

$$n_i\, u\, t = c_{RM}\, x_a(t) \qquad [A.6.5]$$

$$x_a(t) = \frac{n_i u t}{c_{RM}} < d_b \qquad [A.6.6]$$

The effluent concentration starts to increase as third layer disappears. Since the thickness of second layer is small, therefore:

$$x_a(t) = \frac{n_i u T_b}{c_{RM}} \sim d_b \qquad [A.6.7]$$

This justifies equation [5.18] for critical barrier thickness.

A.7. Appendix 7: Calcite Precipitation

The formation of $CaC0_3$ deposit is possible due to the reaction:

$$H_2CO_3 + Ca(OH)_2 = CaCO_3 + 2H_2O$$

There is a danger that $CaCO_3$ microcrystal can block the barrier. This reaction demonstrated that $Ca(OH)_2$ disappears, i.e. pH decreases. On other hand, the initial high pH enhances calcite precipitation.

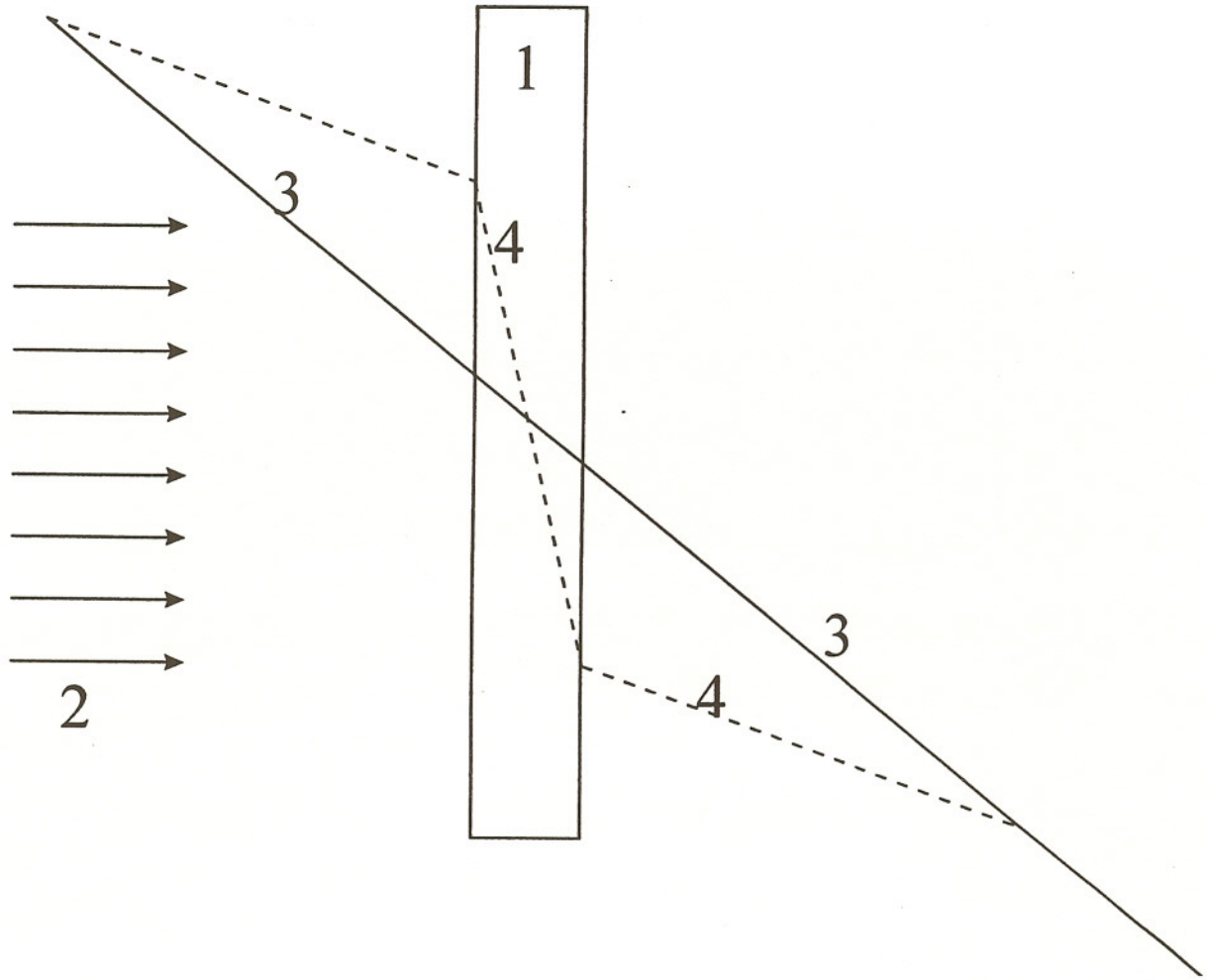

Hydraulic head distribution before, inside and behind a barrier. [1. Barrier, 2. GW stream, 3 Hydraulic head distribution at $K_b = K_a$, 4. Hydraulic head distribution at $K_b < K_a$, K_a = hydraulic conductivity of aquifer, K_b = hydraulic conductivity of barrier]

Figure A.2.1: Schematic illustration of bypassing mechanism

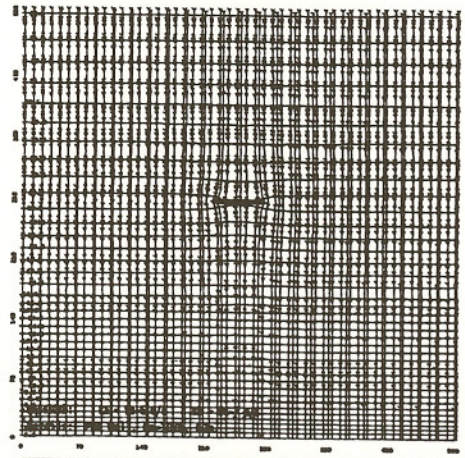

(s) Ka=10Kb, Length 60

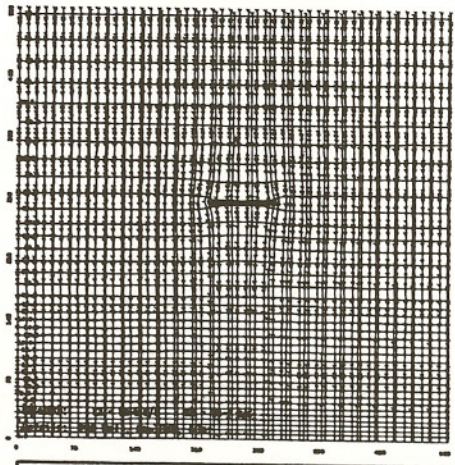

(t) Ka=10Kb, Length 80

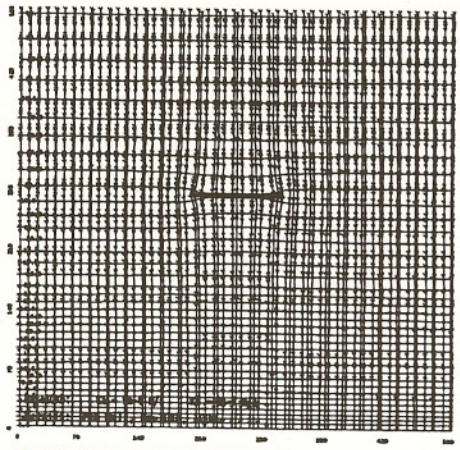

(u) Ka=10Kb, Length 100

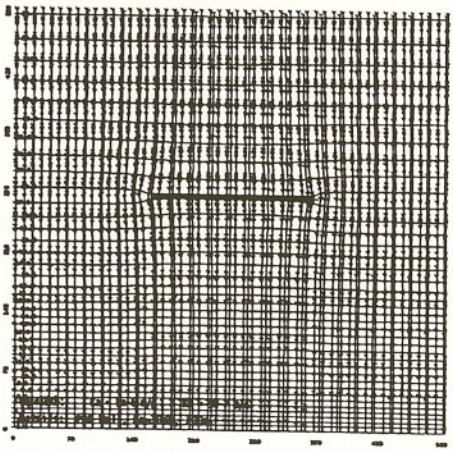

(v) Ka=10Kb, Length 200

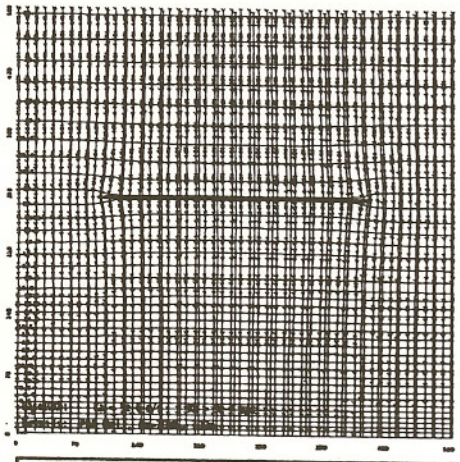

(w) Ka=10Kb, Length 300

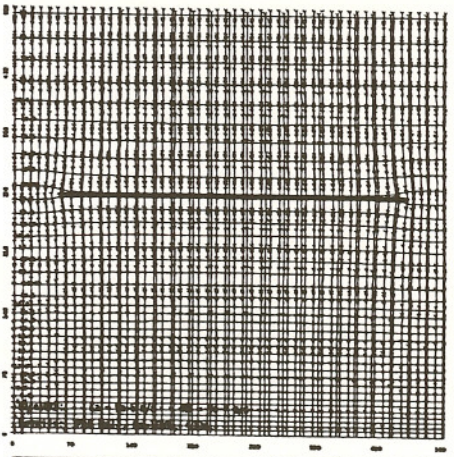

(x) Ka=10Kb, Length 400

Figure A.2.2: Visual modflow runs for varying lengths of barrier (43)

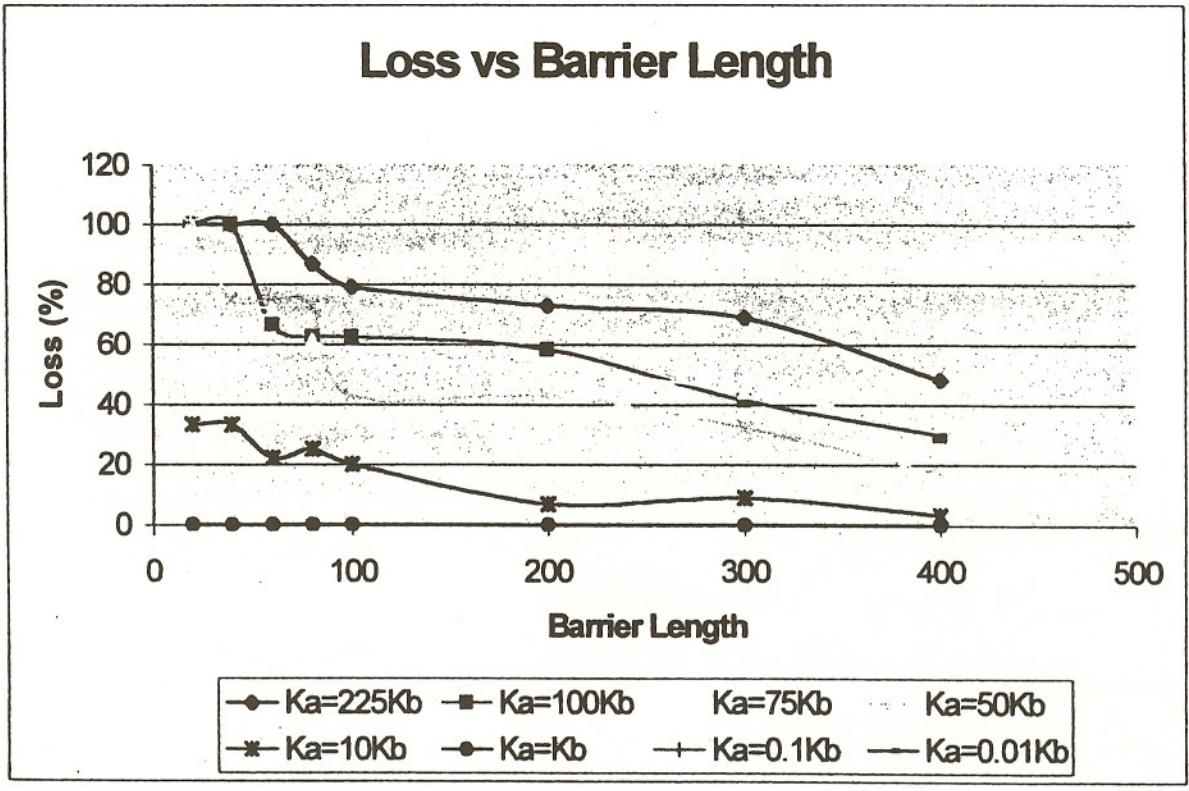

Figure A.2.3: Contaminant loss as a function of barrier length for different values of K_a/K_b

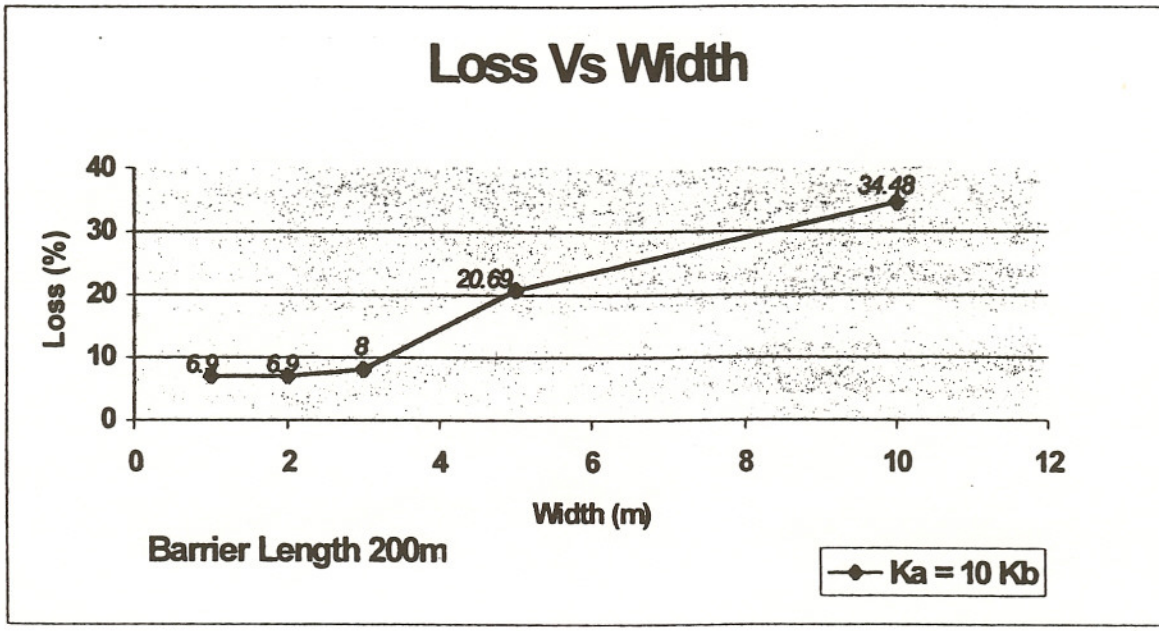

Figure A.2.4: Contaminant loss as a function of barrier width (barrier length = 200 m and $K_a = 10\ K_b$)

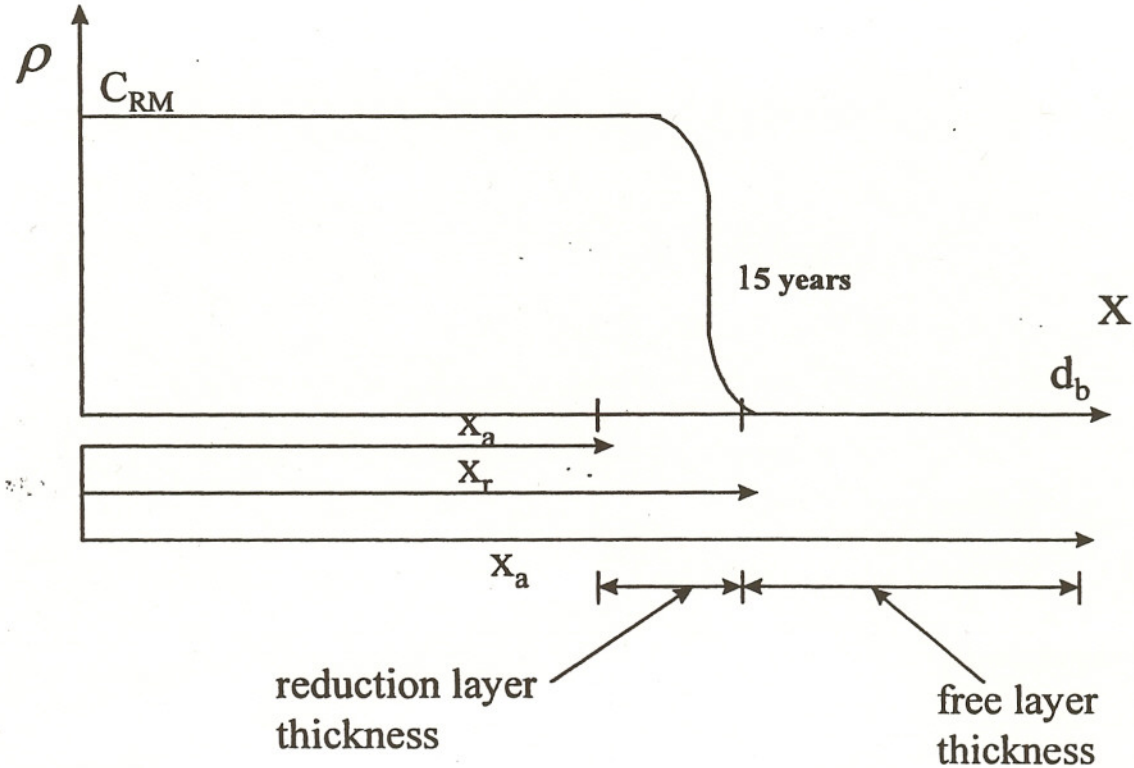

[$X_a(t)$ = current thickness of accumulation layer, $X_r(t)$ = the mobile boundary between reduction layer and third layer, $(X_r - X_a)$ = the thickness of the reduction layer, $(d_b - X_r)$ = the thickness of third (almost free) layer]

Figure A.6.1: Three-layer model of chromium accumulation dynamics in PRB

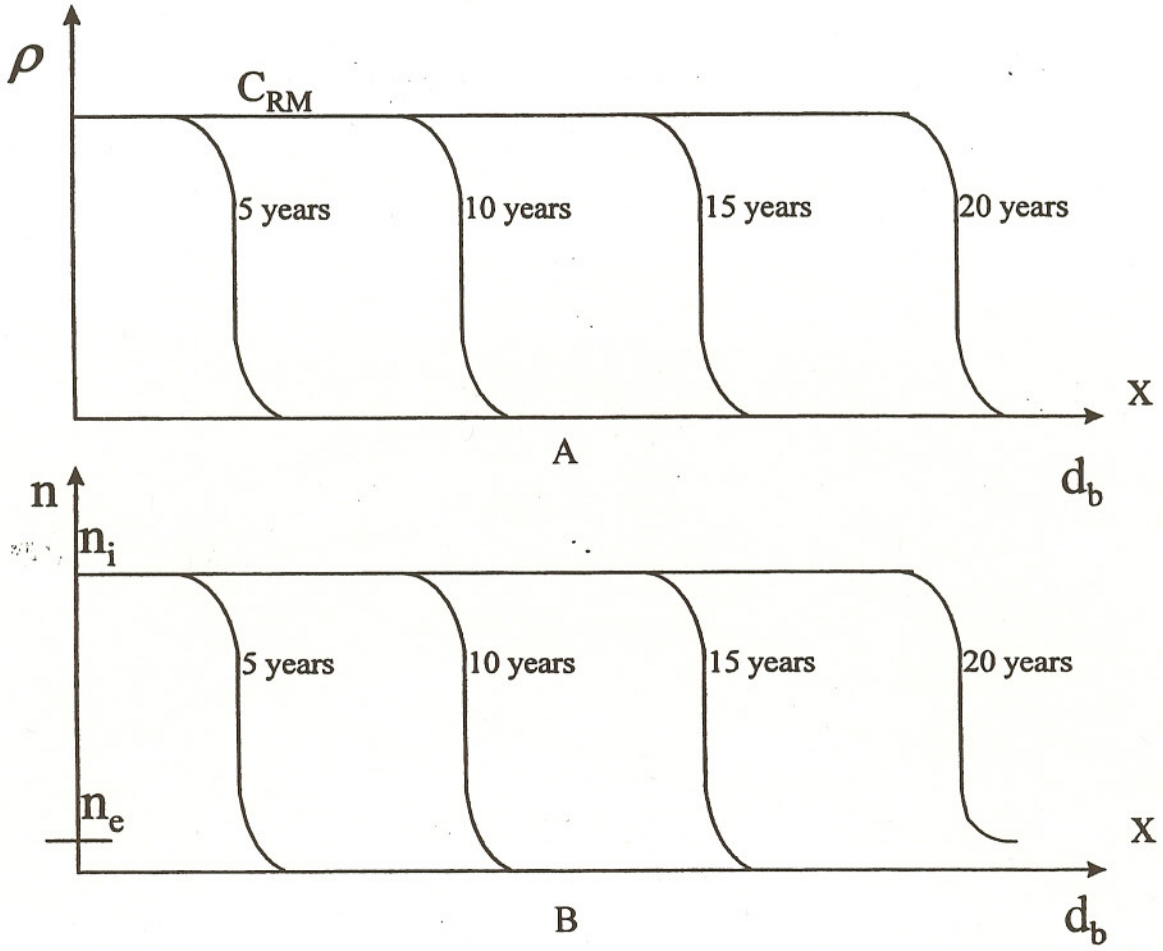

A. The accumulated Cr(III) mass distribution, $\rho(x)$ across a barrier with thickness, d_b for duration from 5 to 20 years; 'x' is the distane from the barrier front (upstream) surface.

B. The dissolved chromium distribution n(x) across the barrier. $n_{x=0} = n_i$, $n_{x=d} = n_e$, n_i and n_e are the influent and the effluent concentrations.

The complete passivation zone with the maximum accumulated chromium, ρ_{max} is seen in Fig. 'A'. Its length extends at constant rate. There is no dissolved chromium reduction within the passivation layer. As a result, the influent concentration is preserved within this passivated layer. After 20 years, the completed passivated zone comprises the entire barrier volume. The reduction takes place in the thin zone near the back (downstream) side of the barrier and correspondingly, concentration (n) decreases in this thin zone only.

Figure A.6.2: Illustration of reactive barrier performance during 20 years